

# Quantum quenches of holographic plasmas

Alex Buchel,<sup>1,2</sup> Luis Lehner,<sup>1</sup> Robert C. Myers,<sup>1</sup> and Anton van Niekerk<sup>1,3</sup>

<sup>1</sup> *Perimeter Institute for Theoretical Physics  
Waterloo, Ontario N2J 2W9, Canada*

<sup>2</sup> *Department of Applied Mathematics, University of Western Ontario  
London, Ontario N6A 5B7, Canada*

<sup>3</sup> *Department of Physics & Astronomy and Guelph-Waterloo Physics Institute  
University of Waterloo, Waterloo, Ontario N2L 3G1, Canada*

## Abstract

We employ holographic techniques to study quantum quenches at finite temperature, where the quenches involve varying the coupling of the boundary theory to a relevant operator with an arbitrary conformal dimension  $2 \leq \Delta \leq 4$ . The evolution of the system is studied by evaluating the expectation value of the quenched operator and the stress tensor throughout the process. The time dependence of the new coupling is characterized by a fixed timescale and the response of the observables depends on the ratio of the this timescale to the initial temperature. The observables exhibit universal scaling behaviours when the transitions are either fast or slow, *i.e.*, when this ratio is very small or very large. The scaling exponents are smooth functions of the operator dimension. We find that in fast quenches, the relaxation time is set by the thermal timescale regardless of the operator dimension or the precise quenching rate.

February 14, 2013

# Contents

<b>1</b>	<b>Introduction</b>	<b>3</b>
<b>2</b>	<b>Holographic model</b>	<b>5</b>
<b>3</b>	<b>Solutions to the equations</b>	<b>8</b>
3.1	Static solutions . . . . .	8
3.2	Time-dependent solutions . . . . .	10
<b>4</b>	<b>Fefferman-Graham coordinates</b>	<b>12</b>
<b>5</b>	<b>Holographic renormalization</b>	<b>13</b>
<b>6</b>	<b>Temperature and entropy density</b>	<b>16</b>
6.1	Final temperature . . . . .	17
6.2	Entropy production during the quench . . . . .	20
6.3	Reverse quenches . . . . .	22
<b>7</b>	<b>Numerical procedure</b>	<b>24</b>
<b>8</b>	<b>Slow quenches and the adiabatic limit</b>	<b>26</b>
<b>9</b>	<b>Results</b>	<b>29</b>
9.1	Response for fast quenches . . . . .	30
9.2	Universal behaviour for fast quenches . . . . .	34
9.3	Response for slow quenches . . . . .	36
9.4	Excitation and relaxation times . . . . .	38
9.5	Behaviour of the energy and pressure . . . . .	41
<b>10</b>	<b>Discussion</b>	<b>42</b>
<b>A</b>	<b>Coefficients in the metric solution</b>	<b>46</b>
<b>B</b>	<b>Coefficients in the Fefferman-Graham coordinates</b>	<b>48</b>
B.1	The time and radial coordinates . . . . .	48
B.2	The metric . . . . .	50
B.3	The scalar field . . . . .	52

## 1 Introduction

Recent advances in cold atom experiments have stimulated a vigorous research program into quantum quenches, processes in which the physical couplings of a quantum system are abruptly changed [1]. The basic motivation is to understand the organizing principles governing the far-from-equilibrium behaviour of such systems. Although such quenches are well understood in the context of quantum mechanics [2], much less is known about such processes in quantum field theories. Theoretical progress has been made for a variety of systems, including two-dimensional conformal field theories, (nearly) free field theories and integrable models – *e.g.*, see [3,4]. However, broadly applicable theoretical techniques, which provide an efficient description of these quenches, remain to be found.

Gauge/gravity duality [5] provides a remarkable new approach to studying certain strongly coupled field theories. Of course, in this framework, questions about the field theory are recast into questions about gravity in one higher dimension. These holographic models seem to be especially well suited for the study of quantum quenches since, with relatively modest efforts, one is able to study strongly coupled quantum field theories, real-time processes and systems at finite temperature, as well as allowing for analysis in general spacetime dimensions. Hence holographic techniques have recently been applied to the study of quantum quenches [6] and the related issue of ‘thermalization’ [7,8]. However, given the complexities of the bulk description of rapid changes in the boundary theory, numerical relativity is increasingly being applied to study these far-from-equilibrium processes [9,10] — see also [11].

In this paper, we extend the calculations presented in [12], in which the gauge/gravity duality was used to study ‘thermal quenches’ in a plasma of the strongly coupled  $\mathcal{N} = 2^*$  gauge theory. More specifically, [12] studied the response of an initial thermal equilibrium state to variations of the coupling of the boundary theory to either a dimension two or three operator. The analysis was restricted to a high temperature regime where the calculations were carried out to leading order in  $m/T \ll 1$ . Here  $m$  is the relevant mass scale introduced by the new coupling. In the present case, we extend these holographic calculations to consider quenches made by coupling to a relevant operator with an arbitrary conformal dimension in the range  $2 \leq \Delta \leq 4$ .

The behaviour of the strongly coupled boundary theory in the present quenches is very similar to that found in [12]. In fact, for many of the results, we are able to identify a simple function of the conformal dimension which interpolates between the different cases which are explicitly studied both here and in [12]. For example, we find that in fast quenches, the increase in the energy density scales like  $(T_i/\Delta t)^{2\Delta-4}$ , where  $T_i$  is the initial temperature and  $\Delta t$  is the timescale over which the new coupling is turned on — fast quenches are then those for which  $T_i/\Delta t \gg 1$ .

The remainder of the paper is organized as follows: In section 2, we describe the holographic model which is used to study our quenches and derive the gravitational equations that are to be solved. Next we examine solutions of these equations in section 3. In particular, by restricting our attention to the high temperature regime, we show that to leading order we only need to solve the linearized equation for the bulk scalar. We also consider the asymptotic boundary expansion for these solutions in Eddington-Finkelstein coordinates. In section 4, we translate the latter expansion to Fefferman-Graham coordinates, which are more suitable to study physical observables in the boundary theory. In section 5, after finding the counterterms that renormalize the bulk action, we find expressions for the expectation value of the stress-energy tensor and the quenched operator in terms of gravitational variables. We also show that these observables obey the expected Ward identities. In section 6, we identify the appropriate translation between the gravitational variables and quantities in the boundary theory. This dictionary allows us to write expressions for the entropy production and the change in other thermodynamic quantities induced by the quench. Section 7 provides a brief description of our numerical procedure. In section 8, we provide an independent analysis of the response in the slow quench limit, which later provides a check of our numerical results. We present and discuss various aspects of our numerical solutions in section 9. We conclude with a summary of the results and further comments in section 10. Finally, there are various appendices describing certain technical details. Appendix A presents explicit coefficients for the leading terms in the asymptotic of the expansion in section 3. Similarly, appendix B presents coefficients for the asymptotic expansions appearing in section 4. Finally, appendix C describes the variations of the renormalized bulk action constructed in section 5, which yield the expectation value of the stress tensor and the quenched operator.

## 2 Holographic model

We will apply holographic techniques to study quantum quenches in a strongly coupled four-dimensional QFT. The quantum quench is implemented by adding a relevant operator with time-dependent coupling to the Lagrangian of the QFT, as follows [12]:

$$\mathcal{L}_0 \rightarrow \mathcal{L}_0 + \lambda(t) \mathcal{O}_\Delta. \quad (2.1)$$

In our calculations, the theory described by  $\mathcal{L}_0$  is in fact a conformal field theory. The operator  $\mathcal{O}_\Delta$  is relevant, meaning that it has conformal dimension  $\Delta < 4$ . We will only consider  $\Delta > 2$  here, as natural in our holographic framework — see below. In our analysis, we start with the theory in a thermal state with  $\lambda = 0$  and quench the system by switching on the coupling to some non-zero value. To further simplify our analysis, we will focus on quenches in the high temperature regime, where the temperature  $T$  provides the dominant scale in the problem. That is, we will only study quenches where  $\lambda \ll T^{4-\Delta}$  at all stages. Note, however, that we will allow the rate of change of coupling  $\lambda$  to be arbitrarily large. In particular, we allow  $\partial_t \lambda(t) \gtrsim T^{5-\Delta}$ .

As the unperturbed QFT is a four-dimensional conformal field theory, the gravitational dual of the vacuum state is five-dimensional anti-de Sitter ( $\text{AdS}_5$ ) spacetime. Since we are interested instead in a thermal state of the boundary CFT, the appropriate dual spacetime is an asymptotically  $\text{AdS}_5$  planar black hole [13] — we consider the boundary QFT in  $R^{1,3}$ , hence the ‘planar’ geometry for the black hole horizon. Switching on the coupling  $\lambda$  is dual to switching on a massive scalar field in the gravitational theory. More precisely, we are modifying the asymptotic boundary conditions for the bulk scalar field in a way that matches the profile  $\lambda(t)$ . Using holographic methods, we can easily determine the response of the QFT by examining the response of the scalar, which yields  $\langle \mathcal{O}_\Delta \rangle$ , as well as the response of the spacetime metric, which yields the energy density, pressure and entropy density of the boundary field theory. Since we are considering the high temperature regime, our calculations will be perturbative in the amplitude of the bulk scalar. That is, the scalar will only produce ‘small’ perturbations on the  $\text{AdS}_5$  black hole background.

The dimension  $\Delta$  of the operator  $\mathcal{O}_\Delta$  is related to the  $\text{AdS}$  length scale  $L$  and the mass  $m$  of the bulk scalar field by [14]

$$\Delta = 2 + \sqrt{4 + L^2 m^2}. \quad (2.2)$$

Notice that a relevant operator is dual to a scalar field with  $m^2 \leq 0$ . Of course, such a

tachyonic mass is still consistent in five-dimensional AdS space as long as it respects the Breitenlohner-Freedman bound [15], *i.e.*,  $m^2 \geq -4/L^2$ . In eq. (2.2), this imposes the constraint  $\Delta \geq 2$ . The unitarity bound for a scalar operator in the four-dimensional CFT allows for  $\Delta \geq 1$ , however, to study operators in the range  $2 > \Delta \geq 1$ , we must use the ‘alternative quantization’ of the dual bulk scalar set forward in [16]. However, we will not consider this possibility in the following and restrict our attention to  $\Delta > 2$ .

The dual gravitational theory is Einstein gravity coupled to a cosmological constant and a massive scalar field, *i.e.*,

$$S_{bulk} = \frac{1}{16\pi G_N^{(5)}} \int d^5x \sqrt{-g} \left( R + 12 - \frac{1}{2} (\partial\Phi)^2 - \frac{1}{2} m^2 \Phi^2 \right). \quad (2.3)$$

Since Newton’s constant appears in an overall factor in front of the action, the scalar field  $\Phi$  is dimensionless. Further, we have also implicitly set the AdS curvature scale to one, *i.e.*,  $L = 1$ , as can be inferred from the cosmological constant term. With this convention, it follows that  $m^2$  will also be a dimensionless number, which is implicitly given in units of  $1/L^2$ . As explained in [12], the scalar field might have further interactions, *e.g.*, a  $\Phi^4$  potential, but any such higher order terms will not play a role in the following analysis describing the high temperature regime.

As an aside, let us comment that it is natural to think of the unperturbed boundary theory as the  $\mathcal{N} = 4$  super-Yang-Mills (SYM) theory, in the limit of large  $N_c$  and large ’t Hooft coupling. In this case, our conventions are such that the five-dimensional Newton’s constant is given by

$$G_N^{(5)} \equiv \frac{\pi}{2 N_c^2}. \quad (2.4)$$

However, we are slightly liberal in our analysis here in that we allow the conformal dimensions of  $\mathcal{O}_\Delta$  to take arbitrary values, rather than restricting ourselves to the spectrum of  $\mathcal{N} = 4$  SYM. In this more general context, we can relate Newton’s constant to the central charge of the boundary CFT with

$$C_T \equiv \frac{5}{\pi G_N^{(5)}}. \quad (2.5)$$

where  $C_T$  is the central charge defining the leading singularity in the two-point correlator of the stress tensor — *e.g.*, see [17].

Varying the action (2.3) with respect to the metric  $g$  and the scalar field  $\Phi$ , one

obtains respectively Einstein's equations and the curved-space Klein-Gordon equation

$$0 = E_{\mu\nu} \equiv R_{\mu\nu} - \frac{1}{2} \partial_\mu \Phi \partial_\nu \Phi - g_{\mu\nu} \left( \frac{1}{2} R + 6 - \frac{1}{4} (\partial\Phi)^2 - \frac{1}{4} m^2 \Phi^2 \right), \quad (2.6)$$

$$0 = \frac{1}{\sqrt{-g}} \partial_\mu (\sqrt{-g} g^{\mu\nu} \partial_\nu \Phi) - m^2 \Phi. \quad (2.7)$$

We express our metric ansatz using infalling Eddington-Finkelstein (EF) coordinates

$$ds^2 = -A(v, y) dv^2 + \Sigma^2(v, y) d\vec{x}^2 + 2 dv dy, \quad (2.8)$$

as was used in [9, 12, 18] in the context of holographic thermal systems. For the scalar in this background, we take  $\Phi = \Phi(v, y)$  (*i.e.*, it is independent of the spatial directions  $x^i$ ). This choice allows us to describe homogeneous quenches where the coupling  $\lambda$  is spatially constant but varies in time. The above is a convenient gauge (2.8) for numerically evolving the scalar field within a characteristic formulation. The resulting radial vector  $\frac{\partial}{\partial y}$  is null and all points on a line with constant  $v$  (and  $x^i$ ) are causally connected. The resulting system of (partial differential) equations provide a nested system of (with both radial and time integrations) that can be evolved the spacetime radially from the boundary at  $y = \infty$  inwards and in forward in time. We will return to this discussion when we describe the numerics in section 7.

With this metric ansatz (2.8), the Klein-Gordon equation (2.7) and Einstein's equations (2.6) become [12]

$$0 = 2\Sigma\partial_y(\dot{\Phi}) + 3(\partial_y\Sigma)\dot{\Phi} + 3\dot{\Sigma}\partial_y\Phi - m^2\Sigma\Phi, \quad (2.9)$$

$$0 = \Sigma\partial_y(\dot{\Sigma}) + 2\dot{\Sigma}\partial_y\Sigma - 2\Sigma^2 + \frac{1}{12}m^2\Phi^2\Sigma^2, \quad (2.10)$$

$$0 = 4 + \partial_y^2 A - \frac{12}{\Sigma^2}\dot{\Sigma}\partial_y\Sigma + \dot{\Phi}\partial_y\Phi - \frac{1}{6}m^2\Phi^2, \quad (2.11)$$

$$0 = \ddot{\Sigma} - \frac{1}{2}\dot{\Sigma}\partial_y A + \frac{1}{6}\Sigma(\dot{\Phi})^2, \quad (2.12)$$

$$0 = \partial_y^2 \Sigma + \frac{1}{6}\Sigma(\partial_y\Phi)^2, \quad (2.13)$$

where we have defined for any function  $h(v, y)$ ,

$$\dot{h} \equiv \partial_v h + \frac{1}{2} A \partial_y h. \quad (2.14)$$

More precisely, the above equations are obtained as:

- Eq. (2.9) is equivalent to the Klein-Gordon equation (2.7) multiplied by  $\Sigma$ .

- Eq. (2.10) corresponds to the combination

$$\frac{1}{3}\Sigma^2 E_{vy} + \frac{1}{6}A\Sigma^2 E_{yy} = 0. \quad (2.15)$$

- Eq. (2.11) corresponds to the combination

$$\frac{1}{3\Sigma^2} (6E_{ii} - 8\Sigma^2 E_{vy} - 4A\Sigma^2 E_{yy}) = 0. \quad (2.16)$$

Note that  $E_{ii}$  denotes one of the diagonal components of  $E_{\mu\nu}$  with  $\mu = \nu = i$ , *i.e.*, there is no implicit sum over  $i$  in this expression.

- Eq. (2.12) corresponds to the combination

$$-\frac{1}{3}\Sigma E_{vv} - \frac{1}{3}A\Sigma E_{vy} - \frac{1}{12}A^2\Sigma E_{yy} = 0. \quad (2.17)$$

- Eq. (2.13) corresponds to  $\Sigma E_{yy} = 0$ .

Note that eqs. (2.12) and (2.13) are constraint equations, implied by the previous three equations [12].

### 3 Solutions to the equations

#### 3.1 Static solutions

As noted above, because we study quenches of the boundary QFT from an initial thermal state, we consider the dual AdS spacetime initially containing a black hole. With  $\Phi = 0$ , the spacetime will have the static solution

$$\begin{aligned} A(v, y) &= y^2 - \frac{\mu^4}{y^2}, \\ \Sigma(v, y) &= y, \end{aligned} \quad (3.1)$$

where the black hole horizon is located at  $y = \mu$  and the asymptotic boundary of the spacetime is located at  $y = \infty$ . This black hole solution gives the gravity description of the original (conformal) boundary theory in thermal equilibrium. The QFT temperature is given by the temperature of the black hole, namely  $T = \mu/\pi$ .<sup>1</sup>

Now following [12], our analysis will be limited to considering a high temperature regime, where  $\lambda(t) \ll T^{4-\Delta}$ . As noted above, this means that our calculations in the

---

<sup>1</sup>Our conventions below will introduce a small correction to this result – see section 6.



dual gravitational description are perturbative in the amplitude of the bulk scalar. In other words, we assume that the AdS spacetime contains a ‘large’ black hole and the scalar only makes ‘small’ perturbations on this background geometry. If we parameterize the amplitude of scalar field by the small parameter  $\ell$ , it follows from the Einstein equations (2.6) that the scalar only backreacts on the metric at order  $\ell^2$ . At the lowest order in  $\ell$ , the scalar and the metric can therefore be written as [12]

$$\begin{aligned}\Phi(v, y) &= \ell \Phi_p(v, y) + o(\ell^3) , \\ A(v, y) &= y^2 - \frac{\mu^4}{y^2} + \mu^2 \ell^2 A_p(v, y) + o(\ell^4) , \\ \Sigma(v, y) &= y + \mu \ell^2 \Sigma_p(v, y) + o(\ell^4) ,\end{aligned}\tag{3.2}$$

where factors of  $\mu$  were introduced above to make both metric functions,  $A_p(v, y)$  and  $\Sigma_p(v, y)$ , dimensionless.

As a matter of convenience, we now change to the dimensionless coordinates  $\rho \equiv \mu/y$ ,  $\tau \equiv \mu v$ , as well as  $\vec{x}' \equiv \mu \vec{x}$ . For this choice of radial coordinate, the boundary lies at  $\rho = 0$  and the black hole horizon lies at  $\rho = 1$ . The scalar field and the metric coefficients are then written as

$$\begin{aligned}\Phi(\tau, \rho) &= \ell \Phi_p(\tau, \rho) + o(\ell^3) , \\ A(\tau, \rho) &= \mu^2 (\rho^{-2} - \rho^2 + \ell^2 A_p(\tau, \rho) + o(\ell^4)) , \\ \Sigma(\tau, \rho) &= \mu (\rho^{-1} + \ell^2 \Sigma_p(\tau, \rho) + o(\ell^4)) .\end{aligned}\tag{3.3}$$

In these coordinates, the metric then becomes

$$ds^2 = \mu^{-2} (-A(\tau, \rho) d\tau^2 + \Sigma^2(\tau, \rho) d\vec{x}'^2) - 2 \frac{d\tau d\rho}{\rho^2} .\tag{3.4}$$

Note that the factor of  $\mu^{-2}$  cancels with the  $\mu^2$  contained in the metric coefficients  $A$  and  $\Sigma^2$ . The metric, and therefore the equations of motion will be independent of the black hole mass parameter  $\mu$  in these coordinates.

If we consider the Klein-Gordon equation (2.9) to order  $\ell$ , the field  $\Phi_p$  decouples from the metric functions  $A_p$  and  $\Sigma_p$  and we are left with the linearized equation [12]

$$-\frac{m^2 \Phi_p}{\rho} + 3 \partial_\tau \Phi_p - (3 + \rho^4) \partial_\rho \Phi_p - 2 \rho \partial_\tau \partial_\rho \Phi_p + (\rho - \rho^5) \partial_\rho^2 \Phi_p = 0 .\tag{3.5}$$

The metric perturbations can then be determined from eqs. (2.10) and (2.11) at order

$\ell^2$  [12]:

$$0 = [-2(3 - \rho^4) + \rho^2(1 - \rho^4)\partial_\rho^2 + \rho(4\partial_\tau - 4\partial_\rho - 2\rho\partial_\tau\partial_\rho)]\Sigma_p + \rho[2 - \rho\partial_\rho]A_p + \frac{m^2}{6\rho}\Phi_p^2, \quad (3.6)$$

$$0 = 24\left[\partial_\tau - \frac{1}{\rho}(1 - \rho^4)(1 + \rho\partial_\rho)\right]\Sigma_p + 2[6 - 2\rho\partial_\rho - \rho^2\partial_\rho^2]A_p + [2\partial_\tau\Phi_p - (1 - \rho^4)\partial_\rho\Phi_p]\partial_\rho\Phi_p + \frac{m^2}{3\rho^2}\Phi_p^2. \quad (3.7)$$

Again, note that the mass parameter  $\mu$  does not appear in these equations (3.5)–(3.7).

In the case of a static or equilibrium configuration, eq. (3.5) can be solved for the leading order scalar field

$$\begin{aligned} \Phi_p(\rho) = & c_1 \rho^{4-\Delta} {}_2F_1\left(\frac{4-\Delta}{4}, \frac{4-\Delta}{4}, \frac{4-\Delta}{2}, \rho^4\right) \\ & - c_1 \frac{\Gamma\left(\frac{4-\Delta}{2}\right)\Gamma\left(\frac{\Delta}{4}\right)^2}{\Gamma\left(\frac{4-\Delta}{4}\right)^2\Gamma\left(\frac{\Delta}{2}\right)} \rho^\Delta {}_2F_1\left(\frac{\Delta}{4}, \frac{\Delta}{4}, \frac{\Delta}{2}, \rho^4\right), \end{aligned} \quad (3.8)$$

where  ${}_2F_1$  denotes a hypergeometric function. The constant  $c_1$  is arbitrary but the coefficient of the second term above is chosen to ensure regularity of the scalar at the horizon. Separately, both  ${}_2F_1\left(\frac{4-\Delta}{4}, \frac{4-\Delta}{4}, \frac{4-\Delta}{2}, \rho^4\right)$  and  ${}_2F_1\left(\frac{\Delta}{4}, \frac{\Delta}{4}, \frac{\Delta}{2}, \rho^4\right)$  have a logarithmic divergence near  $\rho = 1$  but with the relative factor above, these logarithmic terms cancel in eq. (3.8). This static bulk solution will describe the system (to leading order in  $\ell$ ) after it has equilibrated after the quench with a finite coupling  $\lambda$ . Hence it will be useful to extract the relative magnitude of the normalizable and the non-normalizable modes of the bulk scalar in this new equilibrium configuration — see the next section.

### 3.2 Time-dependent solutions

In this subsection, we write down the asymptotic expansion for the leading order scalar  $\Phi_p(\tau, \rho)$  and metric functions,  $A_p(\tau, \rho)$  and  $\Sigma_p(\tau, \rho)$ , in a time-dependent solution. Note that when  $\Delta \in \mathbb{Z}$  or  $\Delta \in \mathbb{Z}_{n+\frac{1}{2}}$  (e.g.,  $\Delta = 2$  or  $3$  as in [12]), logarithmic terms appear in these asymptotic expansions. However, generically these expansions do not contain any logarithmic terms and this is the case that we consider in the following.

The time-dependent solution  $\Phi_p(\tau, \rho)$  has an asymptotic expansion close to  $\rho = 0$  of the form:

$$\begin{aligned} \Phi_p(\tau, \rho) = & \rho^{4-\Delta} \left( \phi_{(0)}(\tau) + \rho \dot{\phi}_{(0)} + \frac{(2\Delta-7)\rho^2}{4(\Delta-3)} \ddot{\phi}_{(0)} + \frac{(2\Delta-9)\rho^3}{12(\Delta-3)} \dddot{\phi}_{(0)} + o(\rho^4) \right) \\ & + \rho^\Delta \left( \phi_{(2\Delta-4)}(\tau) + \rho \dot{\phi}_{(2\Delta-4)} + \frac{(2\Delta-1)\rho^2}{4(\Delta-1)} \ddot{\phi}_{(2\Delta-4)} + \frac{(2\Delta+1)\rho^3}{12(\Delta-1)} \dddot{\phi}_{(2\Delta-4)} + o(\rho^4) \right), \end{aligned} \quad (3.9)$$

where the coefficients  $\phi_{(0)}$  and  $\phi_{(2\Delta-4)}$  are now functions of  $\tau$ . Here  $\dot{h} \equiv \partial_\tau h$ , for any  $\tau$ -dependent function  $h$ . In the following, we will choose some function for the coefficient of the non-normalizable mode,  $\phi_{(0)}(\tau)$ , and then the normalizable coefficient  $\phi_{(2\Delta-4)}(t)$  is determined by numerically integrating eq. (3.5). However, from the static solution (3.8), we have an analytic solution

$$\text{equilibrium :} \quad \phi_{(2\Delta-4)} = -\frac{\Gamma\left(\frac{4-\Delta}{2}\right) \Gamma\left(\frac{\Delta}{4}\right)^2}{\Gamma\left(\frac{4-\Delta}{4}\right)^2 \Gamma\left(\frac{\Delta}{2}\right)} \phi_{(0)} \quad (3.10)$$

for the late-time configuration describing the boundary theory after it has equilibrated with finite  $\lambda$ .

The solutions for the metric perturbations at order  $\ell^2$  take the form

$$A_p(\tau, \rho) = \sum_{n=4} [a_{2,n}(\tau) \rho^{n-2} + \alpha_{2,n}(\tau) \rho^{2-2\Delta+n} + \beta_{2,n}(\tau) \rho^{2\Delta-6+n}] , \quad (3.11)$$

$$\Sigma_p(\tau, \rho) = \sum_{n=5} [s_{2,n}(\tau) \rho^{n-2} + \sigma_{2,n}(\tau) \rho^{2-2\Delta+n} + \theta_{2,n}(\tau) \rho^{2\Delta-6+n}] , \quad (3.12)$$

where (most of) the coefficients can be determined by solving eqs. (3.6) and (3.7) order by order in powers of  $\rho$ . However, the coefficient  $a_{2,4}$  enters these equations as a free parameter. Now taking the limit  $\rho \rightarrow 0$ , we simplify eq. (2.12) using results for the expansion coefficients from the other equations of motion to produce the following constraint:

$$\dot{a}_{2,4} = \frac{1}{9} \left( \Delta (2\Delta-5) \phi_{(2\Delta-4)} \dot{\phi}_{(0)} - (4-\Delta) (2\Delta-3) \phi_{(0)} \dot{\phi}_{(2\Delta-4)} \right), \quad (3.13)$$

and hence

$$\begin{aligned} a_{2,4}(\tau) = \mathcal{C} - \frac{1}{9} (4-\Delta) (2\Delta-3) \phi_{(0)}(\tau) \phi_{(2\Delta-4)}(\tau) \\ + \frac{2}{3} (\Delta-2) \int_{-\infty}^{\tau} d\tau' \phi_{(2\Delta-4)}(\tau') \dot{\phi}_{(0)}(\tau'), \end{aligned} \quad (3.14)$$

where  $\mathcal{C}$  is an integration constant. Following [12], we will choose  $\mathcal{C}$  at a later stage so that the entropy production in the quench is proportional to  $a_{2,4}(\tau = \infty)$ . Note that since initially we have  $\phi_{(0)}(\tau = -\infty) = 0 = \phi_{(2\Delta-4)}(\tau = -\infty)$ , it follows that  $a_{2,4}(-\infty) = \mathcal{C}$ . Further if we set  $\phi_{(0)}(\tau = \infty) = 1$ , then  $a_{2,4}$  asymptotes to

$$\begin{aligned} a_{2,4}(\infty) &= a_{2,4}(-\infty) - \frac{1}{9} (4 - \Delta) (2\Delta - 3) \phi_{(2\Delta-4)}(\infty) \\ &\quad + \frac{2}{3} (\Delta - 2) \int_{-\infty}^{\infty} d\tau' \phi_{(2\Delta-4)}(\tau') \dot{\phi}_{(0)}(\tau'). \end{aligned} \quad (3.15)$$

All the remaining coefficients appearing in eqs. (3.11) and (3.12) can be determined in terms of  $\phi_{(0)}$ ,  $\phi_{(2\Delta-4)}$  and  $a_{2,4}$ . Explicit expressions of some of the leading coefficients are given in appendix A.

## 4 Fefferman-Graham coordinates

We would like to evaluate the entropy density, the expectation value of the stress-energy tensor and of the operator  $\mathcal{O}_{\Delta}$  in the boundary theory during a quench. Following the standard approach [19–21], we need to vary the on-shell gravitational action (2.3) with respect to the asymptotic boundary value of the appropriate fields — see section C. While EF coordinates are useful for evaluating the equations of motion, they are not as useful for determining the boundary one-point functions. The reason for the latter is that the “radial” direction  $\partial_{\rho}$  is not orthogonal to the spacetime boundary located at  $\rho = 0$ , which is clear from the fact that the metric has off-diagonal  $\tau$  and  $\rho$  components. It will therefore be useful to transform to Fefferman-Graham (FG) coordinates [22], in which the radial coordinate is orthogonal to the boundary of the spacetime. The FG coordinates have a spacelike radial coordinate  $r$  in contrast to the EF coordinates, with the null radial coordinate  $\rho$ . The FG coordinates are more appropriate for holographic renormalization, since we can choose a planar cut-off surface by simply fixing  $r$  to some small parameter  $\epsilon$ .

In FG coordinates, the (asymptotically) AdS spacetime has the line-element

$$ds^2 = \frac{G_{ab}(x, r) dx^a dx^b}{r^2} + \frac{dr^2}{r^2}, \quad (4.1)$$

$a$  and  $b$  running from 0 to 3. By equating this FG line-element (4.1) to the previous EF line-element (3.4) and writing the Eddington-Finkelstein coordinates  $\tau$  and  $\rho$  as

functions of the Fefferman-Graham coordinates  $t$  and  $r$ , we obtain a set of three equations from which we can solve for  $\tau(t, r)$  and  $\rho(t, r)$ , as well as the metric component  $G_{00}$ . The set of equations is

$$0 = \mu^{-2} A \rho^2 \dot{\tau} \tau' + (\dot{\rho} \tau' + \rho' \dot{\tau}) , \quad (4.2)$$

$$-1 = r^2 \left( \mu^{-2} A (\tau')^2 + \frac{2}{\rho^2} \rho' \tau' \right) , \quad (4.3)$$

$$G_{00} = r^2 \left( -\mu^{-2} A \dot{\tau}^2 - \frac{2}{\rho^2} \dot{\tau} \dot{\rho} \right) , \quad (4.4)$$

where primes denote  $\partial_r$  and dots denote  $\partial_t$ . We solve eqs. (4.2) and (4.3) by writing  $\tau$  and  $\rho$  as power series in  $r$ , with  $t$ -dependent coefficients:

$$\begin{aligned} \frac{\tau(t, r)}{\mu} &= t + \sum_{n=1} v_{(n)}(t) r^n + \\ &\ell^2 \left( \sum_{n=5} \vartheta_{(n)}(t) r^n + r^{9-2\Delta} \sum_{n=0} \nu_{(n)}(t) r^n + r^{2\Delta} \sum_{n=1} \omega_{(n)}(t) r^n \right) , \end{aligned} \quad (4.5)$$

$$\begin{aligned} \rho(t, r) &= \mu r + \sum_{n=1} \rho_{(n)}(t) r^n + \\ &\ell^2 \left( \sum_{n=5} \chi_{(n)}(t) r^n + r^{9-2\Delta} \sum_{n=0} \xi_{(n)}(t) r^n + r^{2\Delta} \sum_{n=1} \zeta_{(n)}(t) r^n \right) . \end{aligned} \quad (4.6)$$

Upon solving for the above, we can also determine the metric  $G_{ab}$  and scalar field  $\Phi_p$  in terms of similar asymptotic expansions in  $r$

$$\begin{aligned} G_{ab}(t, r) &= g_{ab}^{(0)} + g_{ab}^{(4)} r^4 \\ &+ \ell^2 \left( \sum_{n=4} c_{(n)ab}(t) r^n + r^{8-2\Delta} \sum_{n=0} d_{(n)ab}(t) r^n + r^{2\Delta} \sum_{n=0} e_{(n)ab}(t) r^n \right) \end{aligned} \quad (4.7)$$

$$\Phi_p(t, r) = \left( r^{4-\Delta} \sum_{n=0} f_{(n)}(t) r^n + r^{\Delta} \sum_{n=0} g_{(n)}(t) r^n \right) . \quad (4.8)$$

Explicit expressions of the leading coefficients are given in appendix B. For an asymptotic solution of the nonlinear equations of motion in FG coordinates, see [23].

## 5 Holographic renormalization

Given the metric and scalar field written in FG coordinates, we must evaluate the on-shell gravitational action (2.3). However, a naive evaluation yields a number of

divergences associated with integrating out to the asymptotic boundary at  $r = 0$ . Hence following the standard approach [19–21], we first regulate the calculation by introducing a cut-off surface  $r = \epsilon$  and then the divergences are eliminated by adding boundary counterterms. Actually these counterterms are added in addition to the usual Gibbons-Hawking-Brown-York term

$$S_{GHB\!Y} = -\frac{1}{8\pi G_N^{(5)}} \int d^4x \sqrt{-\gamma} K \Big|_{r=\epsilon}, \quad (5.1)$$

where  $\gamma_{ab}(\epsilon)$  is the induced metric on the cut-off surface and  $K$  is the trace of the extrinsic curvature of this surface. Recall that in our study, we choose the boundary geometry to be flat, *i.e.*,

$$g_{ab}^{(0)} = \lim_{r \rightarrow 0} G_{ab}(t, r) = \eta_{ab}, \quad (5.2)$$

and so the counterterm action turns out to be

$$S_{count} = \frac{1}{16\pi G_N^{(5)}} \int d^4x \sqrt{-\gamma} \left( -6 - \frac{4-\Delta}{2} \Phi^2 \right. \\ \left. + \frac{1}{4(\Delta-3)} (\partial\Phi)^2 + \frac{1}{24(\Delta-3)} R(\gamma) \Phi^2 \right) \Big|_{r=\epsilon}, \quad (5.3)$$

where  $R(\gamma)$  corresponds to the Ricci scalar constructed with  $\gamma_{ab}$ . The  $(\partial\Phi)^2$  and  $R(\gamma) \Phi^2$  terms only cancel divergences which occur when  $\Delta > 3$  and so they should be discarded when  $\Delta \leq 3$ . Although the term with  $R(\gamma) \Phi^2$  vanishes to leading order when evaluated on a planar cut-off surface, it is required to cancel a divergence that arises in varying the metric to determine the stress tensor [24]. In particular, it cancels a divergent contribution to the pressure  $\mathcal{P}$  for  $\Delta > 3$  at order  $\ell^2$ . Also note that for the special cases  $\Delta = 2, 3$  and  $4$ , there are also further logarithmic and finite counterterms, but we do not concern ourselves with these here. The interested reader can find a complete discussion of these cases in [12, 25].

The holographic action  $S_{reg} = S_{bulk} + S_{GHB\!Y} + S_{count}$  can now be used to calculate the one-point correlators of the stress tensor and operator  $\mathcal{O}_\Delta$ . In order to calculate these expectation values, we need to vary  $S_{reg}$  with respect to the boundary metric and the scalar field, respectively. The details of these calculations are given in appendix C

and the final results are:

$$8\pi G_N^{(5)} \mathcal{E} = \frac{3}{2}\mu^4 - \ell^2\mu^4 \left( \frac{3}{2}a_{2,4} + \frac{1}{6}(2\Delta - 3)(4 - \Delta)\phi_{(0)}\phi_{(2\Delta-4)} \right), \quad (5.4)$$

$$8\pi G_N^{(5)} \mathcal{P} = \frac{1}{2}\mu^4 - \ell^2\mu^4 \left( \frac{1}{2}a_{2,4} - \frac{1}{18}(4\Delta - 9)(4 - \Delta)\phi_{(0)}\phi_{(2\Delta-4)} \right), \quad (5.5)$$

$$16\pi G_N^{(5)} \langle \mathcal{O}_\Delta \rangle = 2\mu^\Delta \ell \alpha_\lambda (\Delta - 2) \phi_{(2\Delta-4)}. \quad (5.6)$$

Here  $\mathcal{E}$  and  $\mathcal{P}$  denote the energy density and pressure in the boundary theory, *i.e.*,  $\langle T^{00} \rangle = \mathcal{E}$  and  $\langle T^{ij} \rangle = \delta^{ij} \mathcal{P}$ . Further,  $\alpha_\lambda$  is a proportionality constant relating the leading coefficient in the expansion (4.8) of the bulk scalar with the coupling in the boundary theory, *i.e.*,  $\ell f_{(0)} = \alpha_\lambda \lambda$ . We fix the precise value of this constant in section 6.1 — see eq. (6.16).

These one-point correlators must respect certain Ward identities [21]. In particular, one has the diffeomorphism Ward identity

$$\partial^i \langle T_{ij} \rangle = \langle \mathcal{O}_\Delta \rangle \partial_j \lambda, \quad (5.7)$$

Of course, when the coupling  $\lambda$  is constant, this expression reduces to the conservation of energy and momentum in the boundary theory. In the present case with a time-dependent coupling, the  $j = t$  component of eq. (5.7) yields

$$\partial_t \mathcal{E} = -\langle \mathcal{O}_\Delta \rangle \partial_t \lambda. \quad (5.8)$$

Here the expression on the right-hand side describes the work done by varying the coupling in the boundary theory.<sup>2</sup> Let us verify that eqs. (5.4) and (5.6) satisfy this constraint: First, comparing the expansions of the bulk scalar in eqs. (3.9) and (4.8) and recalling the relation  $\ell f_{(0)} = \alpha_\lambda \lambda$  from appendix C, we find to leading order

$$\phi_{(0)} = \mu^{\Delta-4} \alpha_\lambda \frac{\lambda}{\ell}. \quad (5.9)$$

Then differentiating eq.(5.4), we find

$$\begin{aligned} 8\pi G_N^{(5)} \partial_t \mathcal{E} &= \ell^2 \mu^4 \left( -\frac{3}{2} \dot{a}_{2,4} - \frac{1}{6} (2\Delta - 3)(4 - \Delta) \left( \dot{\phi}_{(0)} \phi_{(2\Delta-4)} + \phi_{(0)} \dot{\phi}_{(2\Delta-4)} \right) \right) \\ &= -\ell^2 \mu^4 (\Delta - 2) \phi_{(2\Delta-4)} \dot{\phi}_{(0)}, \end{aligned} \quad (5.10)$$

---

<sup>2</sup>Note that a minus sign appears here in accord with our conventions, which differ slightly from those in [12].

where we simplified the expression by substituting for  $\dot{a}_{2,4}$  from eq. (3.13). Now using eqs. (5.6) and (5.9), we see that this expression precisely matches the expected Ward identity (5.8). Let us comment that this match should be no surprise since the constraint (2.12) (which was used to derive eq. (3.13)) reduces to precisely this Ward identity (5.8) on the asymptotic boundary  $r = 0$  [12].

We also have the conformal Ward identify

$$T^a_a = (4 - \Delta) \langle \mathcal{O}_\Delta \rangle \lambda, \quad (5.11)$$

which follows from taking the trace of the stress-energy tensor with eqs. (5.4) and (5.5) and substituting eqs. (5.6) and (5.9). Here we do not find any anomalous terms (at quadratic order in  $\ell$ ), since we are assuming that the operator  $\mathcal{O}_\Delta$  has a fractional conformal dimension. This result can be contrasted with the discussion in [12] which considered  $\Delta = 2$  and 3.

## 6 Temperature and entropy density

In this section we will calculate the temperature of the boundary theory before and after the quench, as well as the entropy produced during the quench. As described above, we are assuming that the quench takes the scalar field from a vanishing initial value with  $\phi_{(0)} = 0$  and  $\phi_{(2\Delta-4)} = 0$  to a final equilibrium solution where  $\phi_{(0)} = 1$  and  $\phi_{(2\Delta-4)} = \phi_{(2\Delta-4)}(\infty)$ . In section 6.3, we will consider ‘reverse’ quenches which instead take the system from  $\phi_{(0)} = 1$  to 0. In our perturbative calculations for high temperature quenches, we find that if the profile for the ‘reverse’ quench is given by  $\tilde{\phi}_{(0)}(\tau) = 1 - \phi_{(0)}(\tau)$ , where  $\phi_{(0)}(\tau)$  describes some ‘forward’ quench, then we find that  $\tilde{\phi}_{(2\Delta-4)}(\tau) = \phi_{(2\Delta-4)}(\infty) - \phi_{(2\Delta-4)}(\tau)$ , where  $\phi_{(2\Delta-4)}(\tau)$  is the response for the corresponding ‘forward’ quench. Similarly, we will find that the entropy production is the same in the forward and reverse quenches. Further, in the case of an adiabatic quench, no entropy is created and the process is reversible.

As discussed in section 3.1, the initial configuration before the quench is the well-known planar AdS black hole described by eq. (3.1). The calculation of the corresponding temperature is a straightforward exercise with the result  $T = \mu/\pi$ . However, recall that in eq. (3.14) we established a convention where  $a_{2,4}(-\infty) = \mathcal{C}$ . That is, our metric perturbation is nonvanishing even at  $\tau = -\infty$ . The effect of this convention is to shift the black hole mass parameter, *i.e.*,  $\mu \rightarrow \mu\xi$  where  $\xi^4 = 1 - \ell^2 a_{2,4}(-\infty)$ .



Hence, to quadratic order in the expansion in  $\ell$ , the initial temperature becomes

$$T_i = \frac{\mu \xi}{\pi} = \frac{\mu}{\pi} \left( 1 - \frac{\ell^2}{4} a_{2,4}(-\infty) \right). \quad (6.1)$$

## 6.1 Final temperature

Next we wish to determine the final equilibrium temperature of the system after the quench has taken place. This calculation is more subtle as with our perturbative calculations, since we will not have the full metric describing the final black hole geometry. Instead then, we turn to the thermodynamics of the boundary theory to determine the final temperature. That is, we will compare the energy density and pressure in QFT variables (already in terms of the final temperature  $T_f$  and the coupling  $\lambda$ ) to the energy density and pressure calculated holographically in terms of gravitational variables. In doing so, we are able to derive meaningful relations between the field theory coupling and temperature and the bulk parameters  $\mu$  and  $\ell$ . Of course, by assuming a form for  $\mathcal{E}$  and  $\mathcal{P}$ , our final temperature and entropy production will necessarily depend on the conventions used to define our coupling. This cannot be helped, because we do not know the Lagrangian for the boundary theory when the quench is by an operator of arbitrary dimension  $\Delta$ . This can be contrasted with the discussion in [12] for the cases of  $\Delta = 2, 3$ , where the exact equilibrium expressions for  $\mathcal{E}$  and  $\mathcal{P}$  are known from [26]. Nonetheless, we will find physically meaningful interpretations for our results.

To begin, we make the following ansatz for the energy density and pressure in the final equilibrium of the boundary theory,

$$\mathcal{E}_f = \mathcal{A} T_f^4 \left( 1 - \alpha_f \left( \frac{\lambda_f}{T_f^{4-\Delta}} \right)^2 \right), \quad (6.2)$$

$$\mathcal{P}_f = \frac{\mathcal{A}}{3} T_f^4 \left( 1 - \left( \frac{\lambda_f}{T_f^{4-\Delta}} \right)^2 \right), \quad (6.3)$$

where  $\lambda_f = \lambda(\tau = \infty)$  denotes the final value of the coupling. To leading order our ansatz reduces to the expressions expected for a conformal theory and is in accord with our analysis, the perturbation of these conformal terms is quadratic in the coupling. Further, we have expressed the perturbations in terms of the dimensionless ratio  $\lambda_f/T_f^{4-\Delta}$ . Setting the pre-factor for this term in the pressure (6.3) really defines our normalization for the coupling. We can compare these expressions with those given

in [12, 26]. For example, we find for  $\Delta = 3$ ,

$$\lambda_f^2 = \frac{2\Gamma\left(\frac{3}{4}\right)^4}{\pi^4} m_f^2, \quad (6.4)$$

where  $m_f$  was the fermion mass in the boundary theory. Using this expression, we can confirm the results derived below for the equilibrium values

of the observables agree with those given in [12, 26].

Now we need to determine the constant of proportionality  $\alpha_f$  in eq. (6.3). To proceed, we only assume that the boundary theory obeys standard thermodynamics, following [27]. First, we write the free energy density as

$$F = \mathcal{E} - T S, \quad (6.5)$$

where  $S$  is the entropy density. In the absence of any chemical potentials,  $F = -\mathcal{P}$ . Therefore combining these expressions with eqs. (6.2) and (6.3), the final entropy density is given by

$$S_f = \frac{\mathcal{A}}{3} T_f^3 \left( 4 - (3\alpha_f + 1) \left( \frac{\lambda_f}{T_f^{4-\Delta}} \right)^2 \right). \quad (6.6)$$

We use the first law of thermodynamics (with fixed volume) to write

$$\frac{d\mathcal{E}_f}{dT_f} = T_f \frac{dS}{dT_f}. \quad (6.7)$$

The left-hand side of eq. (6.7) is

$$\frac{d\mathcal{E}_f}{dT_f} = \mathcal{A} T_f^3 \left( 4 - (2\Delta - 4) \alpha_f \left( \frac{\lambda_f}{T_f^{4-\Delta}} \right)^2 \right)$$

whereas the right-hand side is

$$T_f \frac{dS_f}{dT_f} = \mathcal{A} T_f^3 \left( 4 - \frac{1}{3} (3\alpha_f + 1) (2\Delta - 5) \left( \frac{\lambda_f}{T_f^{4-\Delta}} \right)^2 \right).$$

By comparing these two expressions, we solve for  $\alpha_f$  as

$$\alpha_f = \frac{2\Delta - 5}{3}. \quad (6.8)$$

Note that it may seem that the quench has no effect on the energy density for  $\Delta = \frac{5}{2}$  (when  $\alpha_f = 0$ ), but even in this case, the initial and final temperatures will differ by a

term of order  $\lambda_f^2$ . Hence, there will still be a change in  $\mathcal{E}$  in this case, contained in the  $T_f^4$  term in eq. (6.2).

Next, we compare these results for the boundary theory with the corresponding expression in the gravitational dual. In particular, we would like to find  $\ell$  in terms of the temperature  $T_f$  and the coupling  $\lambda_f$ . However, first we fix the normalization factor  $\mathcal{A}$  appearing in eqs. (6.2) and (6.3). This factor would be the unchanged in the initial equilibrium of the conformal boundary theory, *i.e.*, at  $t = -\infty$ , we would have  $\mathcal{E}_i = \mathcal{A} T_i^4$ . Comparing the latter expression with eq. (5.4) then yields

$$\mathcal{A} T_i^4 = \frac{3}{16\pi G_N^{(5)}} \mu^4 (1 - \ell^2 a_{2,4}(-\infty)) . \quad (6.9)$$

Given the expression for the initial temperature in eq. (6.1), we see that

$$\mathcal{A} = \frac{3\pi^4}{16\pi G_N^{(5)}} . \quad (6.10)$$

Next, we take the trace of the stress tensor in both the field theory and the gravitational dual:

$$(T_{\text{QFT}})^a{}_a = -\frac{2}{3} \mathcal{A} T_f^4 (4 - \Delta) \left( \frac{\lambda_f}{T_f^{4-\Delta}} \right)^2 , \quad (6.11)$$

$$\begin{aligned} (T_{\text{GR}})^a{}_a &= \frac{\mu^4 \ell^2}{8\pi G_N^{(5)}} (4 - \Delta) (\Delta - 2) \phi_{(0)} \phi_{(2\Delta-4)} \\ &\xrightarrow{t \rightarrow \infty} \frac{\mu^4 \ell^2}{8\pi G_N^{(5)}} (4 - \Delta) (\Delta - 2) \phi_{(2\Delta-4)}(\infty) , \end{aligned} \quad (6.12)$$

where  $\phi_{(2\Delta-4)}(\infty)$  is given by eq. (3.10) with  $\phi_{(0)} = 1$ , *i.e.*,

$$\phi_{(2\Delta-4)}(\infty) = -\frac{\Gamma\left(\frac{4-\Delta}{2}\right) \Gamma\left(\frac{\Delta}{4}\right)^2}{\Gamma\left(\frac{4-\Delta}{4}\right)^2 \Gamma\left(\frac{\Delta}{2}\right)} . \quad (6.13)$$

Equating the two expressions above and using eq. (6.10), we find

$$\ell^2 = \frac{1}{(\Delta - 2) |\phi_{(2\Delta-4)}(\infty)|} \left( \frac{\lambda_f}{T_f^{4-\Delta}} \right)^2 + o(\lambda_f^4) , \quad (6.14)$$

to leading order in  $\lambda_f/T_f^{4-\Delta}$ . Note that here we have also used eq. (6.1) to substitute  $\mu^4 = \pi^4 T_f^4 + o(\lambda_f^2)$  since the initial and final temperatures will only differ by  $o(\lambda_f^2)$  in our perturbative calculations. Further, the above expression takes account of the fact

that  $\phi_{(2\Delta-4)}(\infty)$  is always negative in the range of interest, *i.e.*,  $2 < \Delta < 4$  — see eq. (6.13) above. Recalling that we set  $\phi_{(0)}(\infty) = 1$ , we note that implicitly the right-hand side of eq. (6.14) is actually  $\ell^2 \phi_{(0)}^2$  and so this equation fixes the normalization between the leading coefficient in the asymptotic expansion of the bulk scalar and the boundary coupling, *i.e.*,

$$\ell \phi_{(0)} = \frac{1}{\sqrt{(\Delta-2)|\phi_{(2\Delta-4)}(\infty)|}} \frac{\lambda}{T^{4-\Delta}} + o(\lambda^3). \quad (6.15)$$

Alternatively in appendix C, we introduced the proportionality constant  $\alpha_\lambda$  in  $\ell f_{(0)} = \alpha_\lambda \lambda$ . So comparing the expansions of the bulk scalar in eqs. (3.9) and (4.8) using eq. (B.37), we now have

$$\alpha_\lambda = \frac{\pi^{4-\Delta}}{\sqrt{(\Delta-2)|\phi_{(2\Delta-4)}(\infty)|}} + o(\lambda^2), \quad (6.16)$$

where as above, we used  $\mu^4 = \pi^4 T^4 + o(\lambda^2)$ .

## 6.2 Entropy production during the quench

Here we extend the previous analysis to determine the entropy production during the quench. First using the expression for the free energy density (6.5), as well as  $F = -\mathcal{P}$ , we find

$$\frac{S_f}{S_i} = \frac{T_i}{T_f} \frac{\mathcal{E}_f + \mathcal{P}_f}{\mathcal{E}_i + \mathcal{P}_i}. \quad (6.17)$$

Initially the boundary theory is conformal and the vanishing trace of the stress tensor requires  $\mathcal{E}_i = 3\mathcal{P}_i$ . Now the latter can be used to re-express eq. (6.17) as

$$\frac{S_f}{S_i} = \frac{T_i}{T_f} \left( \frac{3}{4} \frac{\mathcal{E}_f}{\mathcal{E}_i} + \frac{1}{4} \frac{\mathcal{P}_f}{\mathcal{P}_i} \right). \quad (6.18)$$

First, we determine the ratio of the temperatures by equating the final energy densities given in terms of the gravitational variables (5.4) and of the boundary theory (6.2). The initial temperature is introduced here by substituting for  $\mu$  using eq. (6.1), which then yields

$$\frac{T_i}{T_f} = 1 + \frac{\ell^2}{4} \left( a_{2,4}(\infty) - a_{2,4}(-\infty) + \frac{2}{9} (2\Delta^2 - 8\Delta + 9) \phi_{(2\Delta-4)}(\infty) \right). \quad (6.19)$$

Now using the expressions for the energy density and pressure in eqs. (5.4) and (5.5) at the initial and final times, we find:

$$\frac{\mathcal{E}_f}{\mathcal{E}_i} = 1 - \ell^2 \left( a_{2,4}(\infty) - a_{2,4}(-\infty) + \frac{1}{9} (2\Delta - 3) (4 - \Delta) \phi_{(2\Delta-4)}(\infty) \right), \quad (6.20)$$

$$\frac{\mathcal{P}_f}{\mathcal{P}_i} = 1 - \ell^2 \left( a_{2,4}(\infty) - a_{2,4}(-\infty) - \frac{1}{9} (4\Delta - 9) (4 - \Delta) \phi_{(2\Delta-4)}(\infty) \right). \quad (6.21)$$

Combining these results in eq. (6.18) then yields

$$\frac{S_f}{S_i} = 1 - \frac{3\ell^2}{4} \left( a_{2,4}(\infty) - a_{2,4}(-\infty) - \frac{2}{9} (\Delta - 3) (\Delta - 1) \phi_{(2\Delta-4)}(\infty) \right). \quad (6.22)$$

Now recall from eq. (3.14) that  $a_{2,4}(-\infty) = \mathcal{C}$ , where the latter is an arbitrary integration constant. Hence following [12], we choose this constant to simplify the above ratio of entropies, *i.e.*,

$$a_{2,4}(-\infty) = -\frac{2}{9} (\Delta - 3) (\Delta - 1) \phi_{(2\Delta-4)}(\infty). \quad (6.23)$$

Hence, after substituting for  $\ell^2$  and  $a_{2,4}(-\infty)$  from eqs. (6.14) and (6.23), respectively, the ratio of the final and initial entropies (6.22) becomes

$$\frac{S_f}{S_i} = 1 + \frac{3 a_{2,4}(\infty)}{4 (\Delta - 2) \phi_{(2\Delta-4)}(\infty)} \left( \frac{\lambda_f}{T_f^{4-\Delta}} \right)^2. \quad (6.24)$$

Further substituting for  $\ell^2$  and  $a_{2,4}(-\infty)$  in eqs. (6.19)–(6.21), we find the change in temperature, energy density and pressure are given by

$$\frac{\Delta T}{T_i} = \left[ \frac{\Delta - 2}{6} + \frac{1}{4} \frac{a_{2,4}(\infty)}{(\Delta - 2) \phi_{(2\Delta-4)}(\infty)} \right] \left( \frac{\lambda_f}{T_f^{4-\Delta}} \right)^2, \quad (6.25)$$

$$\frac{\Delta \mathcal{E}}{\mathcal{E}_i} = \left[ \frac{1}{3} + \frac{a_{2,4}(\infty)}{(\Delta - 2) \phi_{(2\Delta-4)}(\infty)} \right] \left( \frac{\lambda_f}{T_f^{4-\Delta}} \right)^2, \quad (6.26)$$

$$\frac{\Delta \mathcal{P}}{\mathcal{P}_i} = \left[ \frac{2\Delta - 7}{3} + \frac{a_{2,4}(\infty)}{(\Delta - 2) \phi_{(2\Delta-4)}(\infty)} \right] \left( \frac{\lambda_f}{T_f^{4-\Delta}} \right)^2, \quad (6.27)$$

where our notation is *e.g.*,  $\Delta \mathcal{P} = \mathcal{P}_f - \mathcal{P}_i$ .

The second law of thermodynamics demands that the ratio  $S_f/S_i$  must always be greater than one. Hence requiring  $a_{2,4}(\infty) \leq 0$  becomes a test of our numerical solutions and we successfully confirm that this inequality is satisfied in the obtained numerical

solutions. Since  $\phi_{(2\Delta-4)}(\infty)$  is always negative in our analysis (and we restrict our attention to  $\Delta > 2$ ), eqs. (6.25) and (6.26) indicate that the changes in the temperature and the energy density are always positive. However, from eq. (6.27), the change in pressure is only guaranteed to be positive for  $\Delta \geq 7/2$ . Otherwise, the pressure can either increase or decrease depending on the precise value of  $\Delta$  and the magnitude of  $a_{2,4}(\infty)$ . A more detailed discussion is given in section 9.5, where we consider the effect of the numerically determined values of  $a_{2,4}(\infty)$  on the shifts of these quantities.

Another check of the present analysis comes from considering the adiabatic limit. As we discuss in section 8 in this case, the system remains in a quasi-static equilibrium with  $\phi_{(2\Delta-4)}(t) = \phi_{(2\Delta-4)}(\infty) \phi_{(0)}(t)$ . Substituting this expression into eq. (3.15), as well as using the integration constant chosen in eq. (6.23), it is straightforward to show that  $a_{2,4}(\infty)$  vanishes. Hence as expected for an adiabatic transition, no entropy is produced, as discussed in [12].

As a final consistency check, we consider the speed of sound in the thermal plasma, which is given by

$$\begin{aligned} c_s^2 = \frac{d\mathcal{P}}{d\mathcal{E}} &= \left( \frac{d\mathcal{P}}{dT_f} \right) / \left( \frac{d\mathcal{E}}{dT_f} \right) \\ &= \frac{1}{3} - \frac{1}{9} (4 - \Delta) (\Delta - 2) \left( \frac{\lambda_f}{T_f^{4-\Delta}} \right)^2. \end{aligned} \quad (6.28)$$

Note the second term is negative for all  $\Delta$  in the range  $2 < \Delta < 4$ . Hence we find  $c_s^2 < 1/3$ , as required by [28]. While  $c_s^2 = 1/3$  for  $\Delta = 2$  and 4, our analysis only applies for the conformal dimension strictly limited within the range  $2 < \Delta < 4$ .

### 6.3 Reverse quenches

Up until now we have assumed that the quenches begin with the boundary theory being conformal, *i.e.*,  $\lambda = 0$  and then end with some finite  $\lambda$ . In the gravitational description then, they involve some profile  $\phi_{(0)}(\tau)$  which begins with  $\phi_{(0)} = 0$  at  $\tau = -\infty$  and ends with  $\phi_{(0)} = 1$  at  $\tau = \infty$ . In this section, we consider ‘reverse’ quenches in which the coupling is initially finite and is brought down to zero. In particular, we can readily repeat the analysis for reverse quenches where the non-normalizable coefficient of the bulks scalar is chosen to be

$$\tilde{\phi}_{(0)}(\tau) = 1 - \phi_{(0)}(\tau). \quad (6.29)$$

Because our analysis is limited to the perturbative high temperature regime, the equation of motion (3.5) for the bulk scalar is linear and hence we can add any two solutions to produce a third solution. In particular then, adding the scalar field solutions for the forward and reverse quench must yield the equilibrium solution with  $\phi_{(0)}(\tau) = 1$ . Alternatively, the reverse quench produced from eq. (6.29) is simply the equilibrium solution (3.8) (with  $c_1 = 1$ ) minus the time-dependent solution describing the forward quench. In the equilibrium case, the normalizable coefficient in the bulk scalar is  $\phi_{(2\Delta-4)}(\infty)$  and so the corresponding coefficient in the reverse quench must be

$$\tilde{\phi}_{(2\Delta-4)}(\tau) = \phi_{(2\Delta-4)}(\infty) - \phi_{(2\Delta-4)}(\tau), \quad (6.30)$$

where  $\phi_{(2\Delta-4)}(\tau)$  denotes the response produced in the original (forward) quench.

In the reverse quench, the metric coefficient  $\tilde{a}_{2,4}$  still satisfies eq. (3.14) and so we have the solution

$$\begin{aligned} \tilde{a}_{2,4}(\tau) = & \tilde{\mathcal{C}} - \frac{1}{9}(4 - \Delta)(2\Delta - 3)\tilde{\phi}_{(0)}(\tau)\tilde{\phi}_{(2\Delta-4)}(\tau) \\ & + \frac{2}{3}(\Delta - 2)\int_{-\infty}^{\tau} d\tau' \tilde{\phi}_{(2\Delta-4)}(\tau')\dot{\tilde{\phi}}_{(0)}(\tau'). \end{aligned} \quad (6.31)$$

where  $\tilde{\mathcal{C}}$  is a new integration constant. Note that in this case, the second term vanishes for  $\tau \rightarrow \infty$  but as  $\tau \rightarrow -\infty$ , it is proportional to  $\tilde{\phi}_{(2\Delta-4)}(-\infty) = \phi_{(2\Delta-4)}(\infty)$ . Repeating the analysis of the previous section for our reverse quench and demanding that the entropy production is now proportional to  $\tilde{a}_{2,4}$ , we find that the integration constant must be chosen as

$$\tilde{\mathcal{C}} = \frac{1}{3}(\Delta - 2)\tilde{\phi}_{(2\Delta-4)}(-\infty). \quad (6.32)$$

With this choice then, we have

$$\frac{S_f}{S_i} = 1 + \frac{3\tilde{a}_{2,4}(\infty)}{4(\Delta - 2)\tilde{\phi}_{(2\Delta-4)}(-\infty)} \left( \frac{\lambda_f}{T_f^{4-\Delta}} \right)^2. \quad (6.33)$$

Further, when we compare the expression for  $\tilde{a}_{2,4}(\infty)$  with eq. (3.15) for  $a_{2,4}(\infty)$ , it is straightforward to show that these two constants are equal, *i.e.*,

$$\tilde{a}_{2,4}(\infty) = a_{2,4}(\infty), \quad (6.34)$$

just as was found in [12]. Hence comparing to eqs. (6.24) and (6.33) and noting that  $\tilde{\phi}_{(2\Delta-4)}(-\infty) = \phi_{(2\Delta-4)}(\infty)$ , we see that the entropy production is identical in the forward and reverse quenches.

We can also find the changes in the temperature, the energy density and pressure as before:

$$\frac{\Delta T}{T_i} = \left[ -\frac{\Delta-2}{6} + \frac{1}{4} \frac{\tilde{a}_{2,4}(\infty)}{(\Delta-2)\tilde{\phi}_{(2\Delta-4)}(\infty)} \right] \left( \frac{\lambda_f}{T_f^{4-\Delta}} \right)^2, \quad (6.35)$$

$$\frac{\Delta \mathcal{E}}{\mathcal{E}_i} = \left[ -\frac{1}{3} + \frac{\tilde{a}_{2,4}(\infty)}{(\Delta-2)\tilde{\phi}_{(2\Delta-4)}(\infty)} \right] \left( \frac{\lambda_f}{T_f^{4-\Delta}} \right)^2, \quad (6.36)$$

$$\frac{\Delta \mathcal{P}}{\mathcal{P}_i} = \left[ -\frac{2\Delta-7}{3} + \frac{\tilde{a}_{2,4}(\infty)}{(\Delta-2)\tilde{\phi}_{(2\Delta-4)}(\infty)} \right] \left( \frac{\lambda_f}{T_f^{4-\Delta}} \right)^2, \quad (6.37)$$

where again *e.g.*,  $\Delta \mathcal{P} = \mathcal{P}_f - \mathcal{P}_i$ . Comparing these expressions for the reverse quench with the corresponding results in eqs. (6.25)–(6.27) for the forward case, we see that  $a_{2,4}(\infty)$  and  $\tilde{a}_{2,4}(\infty)$  have the same coefficients while the constant terms are equal but with opposite sign. Hence for the reverse quenches, whether any of these physical quantities increases or decreases depends on both the magnitude of  $\tilde{a}_{2,4}(\infty)$  and the value of  $\Delta$  — see section 9.5 for a further discussion. We also note that in the case of an adiabatic quench (see section 8), we find  $a_{2,4}(\infty) = 0$  and hence  $\tilde{a}_{2,4}(\infty) = 0$ . That is, for adiabatic transitions, no entropy is produced. However, we would also find that the changes in the temperature, energy density and pressure are exactly opposite in the forward and reverse cases.

Since the forward and reverse quenches are simply related in our perturbative high temperature analysis, we will continue to focus on the forward quenches in the rest of the paper.

## 7 Numerical procedure

We now briefly describe the numerical simulations which we used to understand the quenches. Essentially we implemented the same approach as in [12], using numerical techniques developed in [29, 30]. For details on our numerical implementation the interested reader can see the appendix in [12]. The primary purpose of our simulations was to find the response  $\phi_{(2\Delta-4)}(\tau)$  for a given source  $\phi_{(0)}(\tau)$ , as described earlier, it is convenient to work with infalling characteristics and in particular we adopt Eddington-Finkelstein coordinates as in eq. (2.8) or (3.4). These coordinates are regular at the horizon allowing us to excise the black hole from the computational domain (by integrating some distance inwards and stopping the integration as this region is causally



disconnected from the outside).

We choose the source term in the asymptotic expansion (3.9) of the bulk scalar to be

$$\phi_{(0)}(\tau) = \frac{1}{2} + \frac{1}{2} \tanh\left(\frac{\tau}{\alpha}\right). \quad (7.1)$$

This describes a family of quenches where, as desired, the source starts at zero in the asymptotic past and ends at one in the asymptotic future. Here  $\alpha$  controls the rate at which the quench takes place. In terms of the dimensionful time, we have  $\tau = \mu v \simeq \mu t$  and hence the timescale on which the transition from zero to finite coupling is made is

$$\Delta t = \frac{\alpha}{\mu} \simeq \frac{\alpha}{\pi T_i}. \quad (7.2)$$

Hence for  $\alpha \gg 1$ , the quenches are ‘slow’ which means that the transition occurs on a timescale that is much longer than the thermal relaxation timescale. Alternatively for  $\alpha \ll 1$ , the quenches are ‘fast’, meaning the transition timescale is much shorter than the thermal timescale. The limit  $\alpha \rightarrow 0$  would correspond to an ‘instantaneous’ quench, *i.e.*,  $\phi_{(0)}$  becomes a step-function. The limit  $\alpha \rightarrow \infty$  corresponds to an adiabatic transition — see section 8. We note that with eq. (7.1), the source profile has a continuous derivative for all time. More general quenches which are not infinitely differentiable with respect to time will be studied in a later paper [31].

Again the goal of our simulations is to find the response  $\phi_{(2\Delta-4)}(\tau)$  for a given source  $\phi_{(0)}(\tau)$ . Practically, it is more convenient to solve the linearized scalar equation (3.5) in terms of  $\hat{\phi}(\tau, \rho)$ , which is defined by

$$\Phi_p(t, \rho) = \rho^{4-\Delta} \left( \phi_{(0)} + \rho \dot{\phi}_{(0)} + \frac{(2\Delta-7)\rho^2}{4(\Delta-3)} \ddot{\phi}_{(0)} + \dots \right) + \rho^\kappa \hat{\phi}(\tau, \rho). \quad (7.3)$$

Here the term in brackets contains the leading terms in the asymptotic expansion (3.9) of  $\Phi_p$ . In particular, we include any terms which are leading compared to  $\rho^\Delta$ . Formally then the leading solution takes the form  $\hat{\phi} = \rho^{\Delta-\kappa} \phi_{(2\Delta-4)} + \dots$  and so the leading behaviour in  $\hat{\phi}$  contains the desired response function. However, as a practical matter, we obtained noticeably better accuracy for  $\phi_{(2\Delta-4)}$  by fitting  $\hat{\phi}$  (at each timestep) with an expansion of the form

$$\hat{\phi}(\tau, \rho) = \epsilon_0 \rho^{4-\Delta-\kappa} + \epsilon_1 \rho^{5-\Delta-\kappa} + \dots + \rho^{\Delta-\kappa} \phi_{(2\Delta-4)} + \delta_n \rho^{4-\Delta-\kappa+n} + o(\rho^{\Delta-\kappa+1}), \quad (7.4)$$

where  $\rho^{4-\Delta-\kappa+n}$  is the next leading order after  $\rho^{\Delta-\kappa}$ . The coefficients  $\epsilon_i$  are, of course, all very small since the terms at these orders are already included in eq. (7.3). The

factor  $\delta_n$  is typically not small, but including this term nonetheless gives better results when fitting  $\phi_{(2\Delta-4)}$ . In the cases that we choose  $\kappa > 4 - \Delta$ , we only include terms in eq. (7.4) with nonnegative powers of  $\rho$ .

We introduce  $\kappa$  for convenience in the fit and choose it so that  $\hat{\phi}$  still vanishes at the asymptotic boundary, *i.e.*,  $\rho = 0$ . We further choose  $\kappa$  so that the relative power of  $\rho$  between the two contributions in eq. (7.3) is an integer, *i.e.*,  $\Delta + \kappa$  is an integer. This ensures that upon substituting into the equation of motion (3.5), after simplification, only integer powers of  $\rho$  appear in the coefficients of  $\hat{\phi}$  and its derivatives, as well as in the source terms. Our choices of  $\kappa$ , for each of the conformal dimensions considered in our simulations, are shown in table 1.

Table 1: Choices made for  $\kappa$  while simulating  $\hat{\phi}(\tau, \rho)$  for various  $\Delta$ .

$\Delta$	7/3	8/3	10/3	11/3	4
$\kappa$	5/3	4/3	5/3	1/3	2

Once the numerical solution has been obtained at each timestep, we fit  $\hat{\phi}$  with a series in  $\rho$  with rational exponents, as described above, to determine the coefficient  $\phi_{(2\Delta-4)}$ . Repeating this process for each timestep then generates the full profile for  $\phi_{(2\Delta-4)}(\tau)$ .

## 8 Slow quenches and the adiabatic limit

In this section, we consider the case where the transition between the initial and final theories is made arbitrarily slow. In fact, we find an analytic solution of  $a_{2,4}$  for such slow quenches below. The results derived from this approach provide an independent check for our numerical solutions — see the discussion in section 10.

Let us first consider the adiabatic limit: Given our choice for the integration constant  $a_{2,4}(-\infty)$  in eq. (6.23), the expression (3.15) for  $a_{2,4}(\infty)$  after equilibration becomes

$$a_{2,4}(\infty) = -\frac{1}{3}(\Delta - 2)\phi_{(2\Delta-4)}(\infty) + \frac{2}{3}(\Delta - 2)\int_{-\infty}^{\infty} d\tau' \phi_{(2\Delta-4)}(\tau') \dot{\phi}_{(0)}(\tau'). \quad (8.1)$$

As noted in [12], in the adiabatic limit, the system remains in a quasi-static equilibrium throughout the transition. Hence the ratio of the normalizable and non-normalizable

coefficients in the bulk scalar are precisely as given in eq. (3.10) at every stage of the transition, *i.e.*,

$$\text{adiabatic :} \quad \phi_{(2\Delta-4)}(\tau) = \phi_{(2\Delta-4)}(\infty) \phi_{(0)}(\tau). \quad (8.2)$$

In this case, the integral in eq. (8.1) becomes

$$\begin{aligned} \int_{-\infty}^{\infty} d\tau' \phi_{(2\Delta-4)}(\tau') \dot{\phi}_{(0)}(\tau') &= \frac{1}{2} \phi_{(2\Delta-4)}(\infty) \int_{-\infty}^{\infty} d\tau' \partial_{\tau'} (\phi_{(0)}(\tau'))^2 \\ &= \frac{1}{2} \phi_{(2\Delta-4)}(\infty). \end{aligned} \quad (8.3)$$

Given this result, we easily see that  $a_{2,4}(\infty)$  (and hence the entropy production) vanishes in the adiabatic limit.

For arbitrarily slow quenches, the response should approach the adiabatic profile (8.2) as a limit. Given the profile in eq. (7.1), this slow limit is achieved by taking  $\alpha$  large. Then following [12], we can write the bulk scalar  $\Phi_p$  in an expansion in inverse powers of  $\alpha$ , *i.e.*,

$$\Phi_p = \phi_{(0)}(\tau) \Phi_e(\rho) + \sum_{n=1}^{\infty} \alpha^{-n} \phi_s^{(n)}(\tau) R_s^{(n)}(\rho), \quad (8.4)$$

where  $\phi_{(0)}(\tau)$  is the profile in eq. (7.1) and  $\Phi_e(\rho)$  is the equilibrium solution given in eq. (3.8) (with  $c_1 = 1$ ). Hence the first term above is the desired solution describing an adiabatic transition, *i.e.*, this term yields the response in eq. (8.2). We have assumed that each of the subsequent terms in the series are separable and this form is easily confirmed, *e.g.*, see below.

Let us solve for the first correction in eq. (8.4),  $\phi_s^{(1)}(\tau) R_s^{(1)}(\rho)$ , since this term produces the leading contribution to  $a_{2,4}$  in the slow quench limit. Substituting our ansatz (8.4) into the decoupled Klein-Gordon equation (3.5), we find at order  $\alpha^{-1}$

$$\begin{aligned} \phi_s^{(1)}(\tau) [-\rho^2 (1 - \rho^4) \partial_{\rho}^2 + \rho (\rho^4 + 3) \partial_{\rho} + m^2] R_s^{(1)}(\rho) \\ = \alpha \dot{\phi}_{(0)} \rho (3 - 2\rho \partial_{\rho}) \Phi_e(\rho). \end{aligned} \quad (8.5)$$

Note that  $\alpha \dot{\phi}_{(0)}$  is order  $\alpha^0$  in our expansion because the derivative of  $\phi_{(0)}$  brings out a factor of  $1/\alpha$ . Now solving eq. (8.5), requires that the time-dependent function takes the form  $\phi_s^{(1)}(\tau) = \alpha \dot{\phi}_{(0)}$  while the radial profile satisfies the inhomogeneous equation:

$$[-\rho^2 (1 - \rho^4) \partial_{\rho}^2 + \rho (\rho^4 + 3) \partial_{\rho} + \Delta(\Delta - 4)] R_s^{(1)}(\rho) = \rho (3 - 2\rho \partial_{\rho}) \Phi_e(\rho). \quad (8.6)$$

The solution to the above equation can be written in series form as

$$R_s^{(1)}(\rho) = \rho^{4-\Delta} \sum_{n=0}^{\infty} a_{(n)} \rho^n + \rho^{\Delta} \sum_{n=0}^{\infty} b_{(n)} \rho^n. \quad (8.7)$$

Here we have two independent integration constants,  $a_{(0)}$  and  $b_{(0)}$ . The first coefficient  $a_{(0)}$  is set to zero, since the order  $\rho^{4-\Delta}$  contribution to  $\Phi_p$  defines the source and we do not want any new sources beyond  $\phi_{(0)}$  to appear at higher orders in the  $1/\alpha$  expansion in eq. (8.4). To determine  $b_{(0)}$ , we demand that  $R_s^{(1)}(\rho)$  is regular on the event horizon at  $\rho = 1$ . To analyze the profile close to the horizon, we make the change of coordinates  $z = 1 - \rho$  and solve for  $R_s^{(1)}(z)$ . Near  $z = 0$ , we may write  $R_s^{(1)}(z)$  as the series

$$R_s^{(1)}(z) = \sum_{n=0}^{\infty} c_{(n)} z^n, \quad (8.8)$$

which includes only the solution that is well-behaved at  $z = 0$ . In this series, we now have the undetermined coefficient  $c_{(0)}$ .

To proceed further, we resorted to solving eq. (8.6) numerically. In particular, we produced independent solutions integrating in from  $z = 1$  (or  $\rho = 0$ ) and integrating out from  $z = 0$  (or  $\rho = 1$ ). Then by matching the two solutions for  $R_s^{(1)}$  at an intermediate point between the asymptotic boundary and horizon, we solved for both  $b_{(0)}$  and  $c_{(0)}$  simultaneously. This shooting method was used to solve for the undetermined coefficients in the cases  $\Delta = \frac{7}{3}, \frac{8}{3}, \frac{10}{3}$  and  $\frac{11}{3}$ . We should emphasize that although this approach is again numerical, it is an independent approach very different in spirit from the numerical approach described previously.<sup>3</sup>

Comparing the present solution with the expansion in eq. (3.9), we see that the corrected response takes the form

$$\phi_{(2\Delta-4)}(\tau) = \phi_{(2\Delta-4)}(\infty) \phi_{(0)}(\tau) - b_{(0)} \dot{\phi}_{(0)}(\tau) + o(1/\alpha^2). \quad (8.9)$$

Again the second term above is of order  $1/\alpha$  because the derivative acting on  $\phi_{(0)}(\tau)$  brings out this factor. Now upon substituting this expression into eq. (8.1), the adiabatic response yields zero and so we are left with

$$\begin{aligned} a_{2,4}(\infty) &= -\frac{2}{3}(\Delta - 2) b_{(0)} \int_{-\infty}^{\infty} d\tau' \dot{\phi}_{(0)}^2(\tau') + o(1/\alpha^2) \\ &= -\frac{2}{9\alpha} (\Delta - 2) b_{(0)} + o(1/\alpha^2), \end{aligned} \quad (8.10)$$

---

<sup>3</sup>It is straightforward to write a formal Green's function solution for eq. (8.6). Given this form of the solution, the coefficient  $b_{(0)}$  can be determined by numerically evaluating a specific integral. The results produced this way agree well with those given in eq. (8.11).

where the final result is produced by inserting eq. (7.1) for  $\phi_{(0)}$ . Hence given the numerical solution for  $b_{(0)}$  for each value of  $\Delta$  listed above, we can determine the leading contribution to  $a_{2,4}$  for slow quenches. Our results are as follows:

$$\begin{aligned}
\Delta = \frac{7}{3} : \quad a_{2,4}(\infty) &= -0.01958 \frac{1}{\alpha}, \\
\Delta = \frac{8}{3} : \quad a_{2,4}(\infty) &= -0.05205 \frac{1}{\alpha}, \\
\Delta = \frac{10}{3} : \quad a_{2,4}(\infty) &= -0.09838 \frac{1}{\alpha}, \\
\Delta = \frac{11}{3} : \quad a_{2,4}(\infty) &= -0.1083 \frac{1}{\alpha}.
\end{aligned} \tag{8.11}$$

These results compare well to our numerical results, as discussed below in section 10.

## 9 Results

We now turn to the results of our numerical simulations. We determined the response functions for various values of  $\alpha$  and with several different masses of the bulk scalar. Explicitly, the scalar masses for which we studied the quenches are:  $m^2 = -\frac{35}{9}$  (with  $\Delta = \frac{7}{3}$ ),  $m^2 = -\frac{32}{9}$  (with  $\Delta = \frac{8}{3}$ ),  $m^2 = -\frac{20}{9}$  (with  $\Delta = \frac{10}{3}$ ) and  $m^2 = -\frac{11}{9}$ . The masses were chosen so that the conformal dimension lies in the desired range  $2 < \Delta < 4$  and so that  $4 - 2\Delta$  is not an integer. The latter ensures that the asymptotic expansion (3.9) for the scalar does not contain any logarithmic terms. We further comment on  $\Delta = 4$  case, which together with results of [12] would form a complete picture of perturbative quenches in strongly couple gauge theories induced by the coupling of a relevant operator.

In subsection 9.1, we extract the response function  $\phi_{(2\Delta-4)}$  for fast quenches (*i.e.*,  $\alpha < 1$ ) from our numerical data for each  $\Delta$ . From that we see that  $a_{2,4}$  and the maximum displacement of  $\phi_{(2\Delta-4)}$  follows a scaling behaviour for fast quenches. In subsection 9.2, we see that the scaling of these quantities follow a universal behaviour, determined by  $\Delta$  and  $\alpha$  only. In subsection 9.3, we show the numerical results for slow quenches (*i.e.*,  $\alpha > 1$ ). We show that for very large  $\alpha$ ,  $\phi_{(2\Delta-4)}$  approaches the adiabatic response (8.2). We also find that  $a_{2,4}$  scales as  $\alpha^{-1}$ , as expected from the analysis in section 8. Finally, in subsection 9.4, we study the excitation times of the response, by considering when it first deviates from the adiabatic response by more than 5% (an arbitrary threshold). We find that for fast quenches, the scaled excitation time  $\tau_{ex}/\alpha$  scales logarithmically with the quenching parameter  $\alpha$ . We also see a universal

behaviour in the slopes  $-\left(\frac{\partial(\tau_{ex}/\alpha)}{\partial \log \alpha}\right)$  in the fast quench limit for fractional  $\Delta$ . In the same subsection we study the relaxation times for the quenches, defined by the last time that  $\phi_{(2\Delta-4)}$  falls below a 5% deviation from its final equilibrium value.

### 9.1 Response for fast quenches

Here we list the results for intermediate to fast quenches (*i.e.*,  $\alpha < 1$ ). We first find the response  $\phi_{(2\Delta-4)}$  and then determine the coefficient  $a_{2,4}(\infty)$  using equation (3.15), as well as the integration constant  $a_{2,4}(-\infty)$  in eq. (6.23). By doing multiple simulations of the time-dependent behaviour of  $\phi_{(2\Delta-4)}$  with increasingly finer discretizations, we can extrapolate for the continuum value of  $a_{2,4}(\infty)$ . Knowing  $a_{2,4}(\infty)$ , we can determine the response of various physical quantities in the boundary theory to the quench, using eqs. (6.24)–(6.27). Note that these results would also apply to the reverse quenches, as discussed in section 6.3. We also study the behaviour of  $\phi_{(2\Delta-4)}$  and  $a_{2,4}(\infty)$  as functions of  $\alpha$ . In the next subsection, we compare this  $\alpha$  dependence for different values of  $\Delta$  and identify the universal behaviour for operators of different dimension.

In figure 1, we plotted  $\phi_{(2\Delta-4)}$  against time for various values of  $\alpha$ . The time is rescaled by a factor of  $1/\alpha$  so that the different plots equilibrate in approximately the same distance on the horizontal axis. In each of the plots, we have also rescaled the vertical axis by  $\alpha^{2\Delta-4}$ . Hence the maximum displacement of  $\phi_{(2\Delta-4)}$  is actually growing with decreasing  $\alpha$ . With the rescaled axes, the peaks corresponding to smaller  $\alpha$  lie close together, which seems to indicate that there is a universal scaling depending on the operator dimension. Further with these scalings, the response seems to converge to a particular limit with decreasing  $\alpha$ . For fast enough quenches, we expect these plots to coincide exactly.

In figure 2, we show a different visualization of the same fast quenches. Here,  $\alpha^{2\Delta-4}\phi_{(2\Delta-4)}$  is plotted as a function of the source  $\phi_{(0)}$ . It is perhaps easier to see the convergence of the faster quenches to a limiting curve. Note that because of the growth of  $\phi_{(2\Delta-4)}$  for fast quenches, the expression (3.15) for  $a_{2,4}(\infty)$  is dominated by the integral. Further the latter can be re-expressed as  $\int_0^1 d\phi_{(0)}\phi_{(2\Delta-4)}$  and so for these fast quenches,  $a_{2,4}(\infty)$  is essentially given by the area under the curves in figure 2.

In figure 3,<sup>4</sup> we see that  $\log(-a_{2,4}(\infty))$  plotted against  $\log \alpha$  tends to a straight line for small values of  $\alpha$ . This indicates that  $a_{2,4}(\infty)$  scales as some power law of the quenching parameter  $\alpha$  for very fast quenches. A fit of this linear behaviour suggests

---

<sup>4</sup>Note that we plot the logarithm of  $-a_{2,4}(\infty)$  since  $a_{2,4}(\infty)$  is always negative.

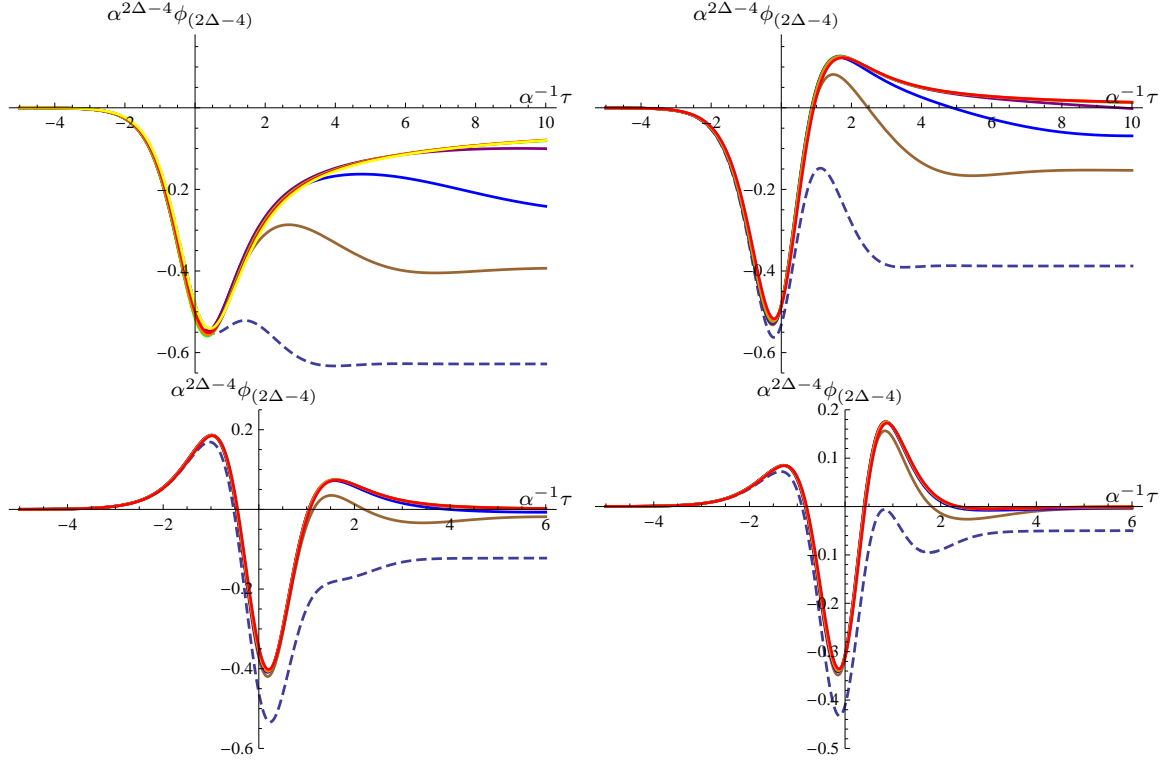


Figure 1: (Colour online) Plots of the response coefficient  $\phi_{(2\Delta-4)}$  for quenches of different speeds, in the fast quench regime. Time is rescaled by a factor of  $1/\alpha$  and the value of  $\phi_{(2\Delta-4)}$  is rescaled by  $\alpha^{2\Delta-4}$ . Clockwise from the top left, the plots are for  $\Delta = 7/3, 8/3, 11/3$  and  $10/3$ . In each case, the response is presented for  $\alpha = 1$  (dashed),  $1/2$  (brown),  $1/4$  (blue),  $1/8$  (purple),  $1/16$  (green),  $1/32$  (orange) and  $1/64$  (red) (as well as  $\alpha = 1/128$  (yellow) for  $\Delta = 7/3$ ).

the slope matches  $4 - 2\Delta$  in each case. The lines shown in the plot are the linear fits through the points corresponding to the three fastest quenches, thus showing the asymptotic behaviour of  $a_{2,4}(\infty)$  for fast quenches. Although it is not shown, for small values of  $\alpha$ , the logarithm of  $\max\{|\phi_{(2\Delta-4)}|\}$  plotted against  $\log \alpha$  also tends to a straight line with the same slope as in the plot of  $\log(-a_{2,4}(\infty))$ .

As discussed in [12,31], the scaling of the response  $\phi_{(2\Delta-4)}$  for fast quenches is more subtle when  $\Delta = 2, 3$  and  $4$ . Specifically, it is rather the ‘subtracted’ response, defined

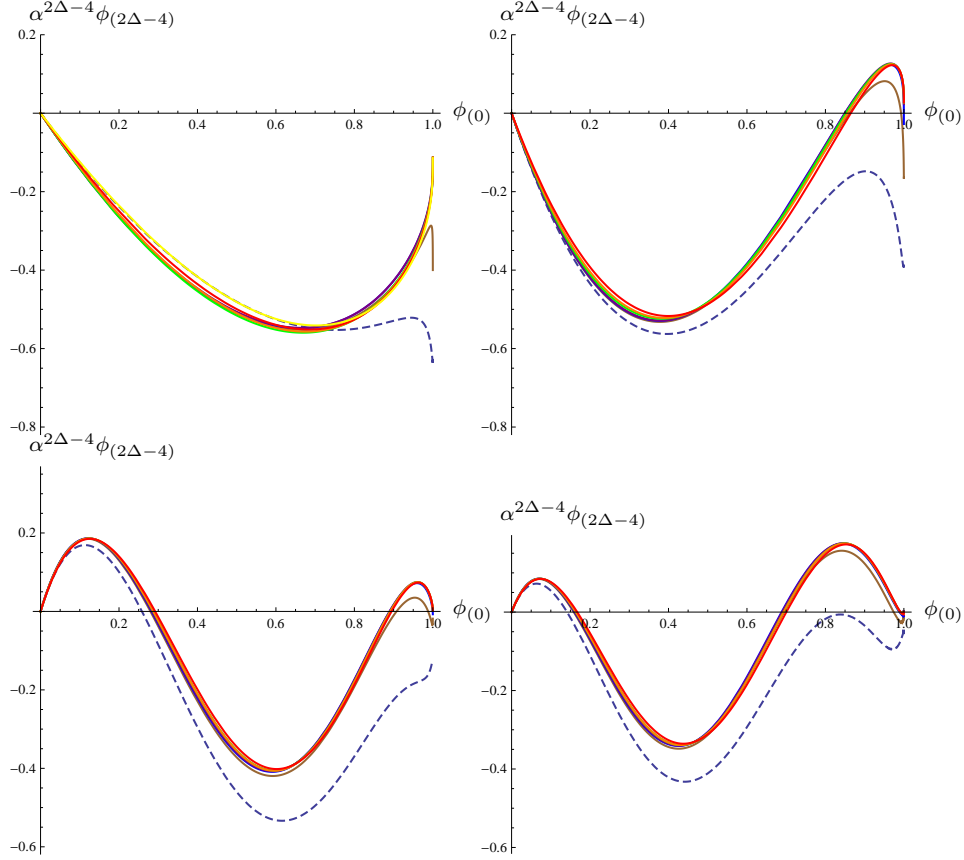


Figure 2: (Colour online) Plots of  $\phi_{(2\Delta-4)}$  for quenches of different speeds, in the fast quench regime.  $\phi_{(2\Delta-4)}$  is rescaled by  $\alpha^{2\Delta-4}$  and is plotted against the actual value of the source  $\phi_{(0)}$ . Clockwise from the top left, the plots are for  $\Delta = 7/3, 8/3, 11/3$  and  $10/3$ . In each case, the response is presented for various values of  $\alpha$ , which are indicated using the same colour scheme as in figure 1.

by

$$\hat{\phi}_{(2\Delta-4)} \equiv \phi_{2\Delta-4} + \begin{cases} \ln \alpha \, \phi_{(0)}, & \text{for } \Delta = 2, \\ \frac{1}{2} \ln \alpha \, \ddot{\phi}_{(0)}, & \text{for } \Delta = 3, \\ -\frac{1}{16} \ln \alpha \, \ddot{\ddot{\phi}}_{(0)}, & \text{for } \Delta = 4, \end{cases} \quad (9.1)$$

which scales faithfully in the limit of fast quenches, *i.e.*,

$$\lim_{\alpha \rightarrow 0} \alpha^{2\Delta-4} \hat{\phi}_{(2\Delta-4)} = \text{constant}. \quad (9.2)$$

Notice, however, that the additional  $\ln \alpha$  terms in  $\phi_{2\Delta-4}$  above do not contribute to



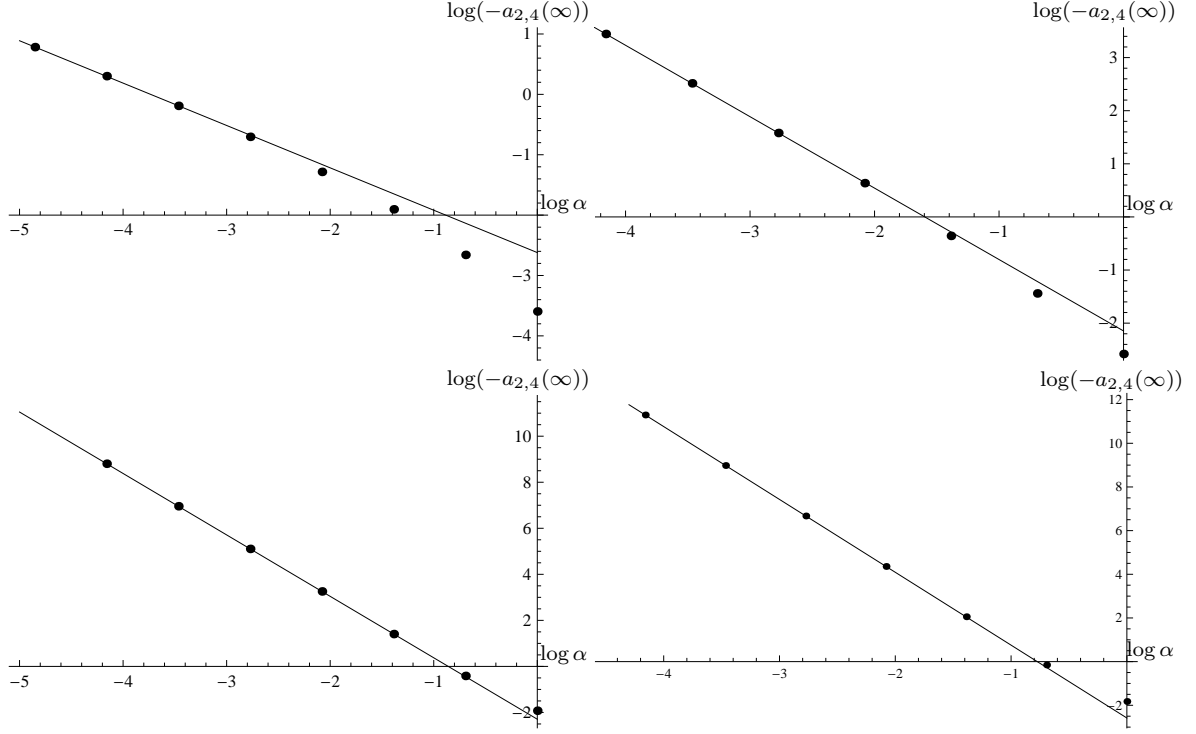


Figure 3: log-log plots for  $-a_{2,4}(\infty)$  versus  $\alpha$  for various  $\Delta$ , in the fast quench regime. The straight lines shown are least-squares fits through the three leftmost data-points in each case. The fact that the plots tend to straight lines for negative values of  $\log \alpha$  means that  $a_{2,4}(\infty)$  scales as a power law for small  $\alpha$ . Clockwise from the top left, the plots are for  $\Delta = 7/3, 8/3, 11/3$  and  $10/3$ .

$a_{2,4}(\infty)$  for  $\Delta = 3$  or  $4$ . For these cases, we have

$$\Delta = 3 : \quad \int_{-\infty}^{\infty} d\tau \, \ddot{\phi}_{(0)}(\tau) \dot{\phi}_{(0)}(\tau) = \left[ \frac{1}{2} \dot{\phi}_{(0)}(\tau)^2 \right]_{-\infty}^{\infty} = 0 \quad (9.3)$$

$$\Delta = 4 : \quad \int_{-\infty}^{\infty} d\tau \, \dddot{\phi}_{(0)}(\tau) \dot{\phi}_{(0)}(\tau) = \left[ \ddot{\phi}_{(0)}(\tau) \dot{\phi}_{(0)}(\tau) - \frac{1}{2} \ddot{\phi}_{(0)}(\tau)^2 \right]_{-\infty}^{\infty} = 0$$

which, as we have indicated, both vanish for a generic source  $\phi_{(0)}$  as long as the profile becomes constant as  $\tau \rightarrow \pm\infty$ . Hence for  $\Delta = 3$  and  $4$ , we still have  $a_{2,4}(\infty) \sim 1/\alpha^{2\Delta-4}$  for fast quenches as  $\alpha \rightarrow 0$ . On the other hand, as shown in [12], the logarithmic term in eq. (9.1) gives the dominant contribution in eq. (3.15) for fast quenches with  $\Delta = 2$  and we have instead

$$a_{2,4}(\infty) = \frac{1}{6} \ln \alpha + o(1), \quad \text{as } \alpha \rightarrow 0. \quad (9.4)$$

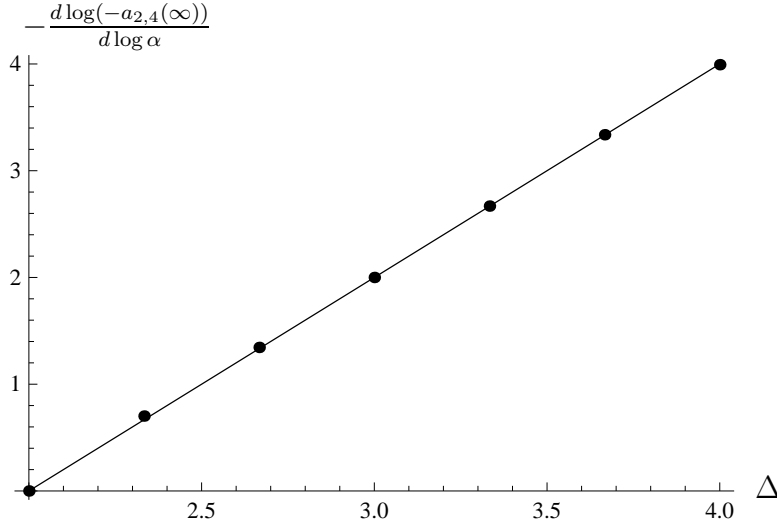


Figure 4: (Colour online) Plot of the asymptotic scaling of  $-a_{2,4}(\infty)$  as a power of  $\alpha$ , in the fast quench limit. The line shown is the predicted theoretical trend  $\frac{-d \log(-a_{2,4}(\infty))}{d \log \alpha} = 2\Delta - 4$ . Points shown are for  $\Delta = 2, 7/3, 8/3, 3, 10/3, 11/3$  and  $4$ . The datapoints for  $\Delta = 2, 3$  are taken from [12]. The datapoint for  $\Delta = 4$  is taken from [31].

## 9.2 Universal behaviour for fast quenches

For fast quenches, our numerics above suggested that  $-a_{2,4}(\infty)$  grows as  $\alpha^{-(2\Delta-4)}$  as  $\alpha$  becomes arbitrarily small. This behaviour is confirmed in figure 4. This plot shows  $\frac{-d \log(-a_{2,4}(\infty))}{d \log \alpha}$  versus  $\Delta$  for  $\Delta = 2, \Delta = 7/3, \Delta = 8/3, \Delta = 3, \Delta = 10/3, \Delta = 11/3$  and  $\Delta = 4$ . The data-points are the slopes of the straight line fits for the plots shown in figure 3. The data-points for  $\Delta = 2$  and  $\Delta = 3$  are taken from [12] while the data-point for  $\Delta = 4$  is taken from [31]. We set the log derivative to zero for  $\Delta = 2$  but, as noted above in eq. (9.4),  $a_{2,4}(\infty)$  actually scales as a logarithm of  $\alpha$  [12].

As well as the individual data-points, we have plotted the line

$$-\frac{d \log[-a_{2,4}(\infty)]}{d \log \alpha} = 2\Delta - 4. \quad (9.5)$$

In fact, a least-squares fit through the data-points yields

$$-\frac{d \log[-a_{2,4}(\infty)]}{d \log \alpha} = 1.99\Delta - 3.96, \quad (9.6)$$

which matches the expected trend within our numerical accuracy. Hence figure 4 confirms the universal scaling

$$|a_{2,4}(\infty)| \propto \frac{1}{\alpha^{2\Delta-4}} \quad (9.7)$$

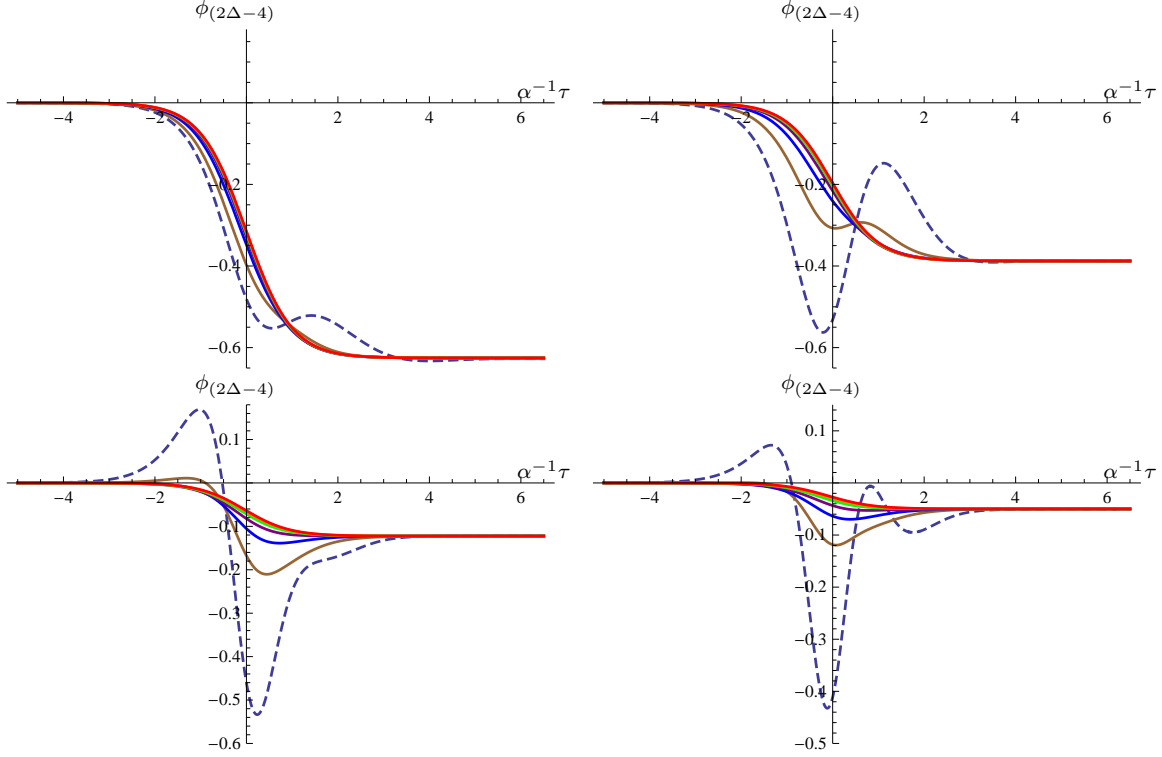


Figure 5: (Colour online) Plots of  $\phi_{(2\Delta-4)}$  for quenches of different speeds in the slow quench regime. Time is rescaled by a factor of  $\alpha^{-1}$  and the value of  $\phi_{(2\Delta-4)}$  is rescaled by  $\alpha^{2\Delta-4}$ . Plots for larger  $\alpha$  follow an inverted tanh-profile more closely, which is a negative constant times the source. Clockwise from the top left, the plots are for  $\Delta = 7/3, 8/3, 11/3$  and  $10/3$ . In each case, the response is presented for  $\alpha = 1$  (dashed), 2 (brown), 4 (blue), 8 (purple), 16 (green), 32 (orange) and 64 (red).

for fast quenches by an operator with  $2 < \Delta \leq 4$ .

As noted above, the maximum displacement of  $\phi_{(2\Delta-4)}$  seems to exhibit the same scaling behaviour as above when  $\Delta$  is fractional. However, as also commented above for  $\Delta = 2$ , both  $a_{2,4}(\infty)$  and  $\phi_{(2\Delta-4)}$  grow as  $-\log \alpha$  for small  $\alpha$  [12]. Similarly, for small  $\alpha$  with  $\Delta = 3$  and 4,  $a_{2,4}(\infty)$  has the above scaling but the maximum displacement of  $\phi_{(2\Delta-4)}$  exhibits an additional  $\log \alpha$  growth on top of this simple scaling — see further discussion around eq. (9.1) and in [31].

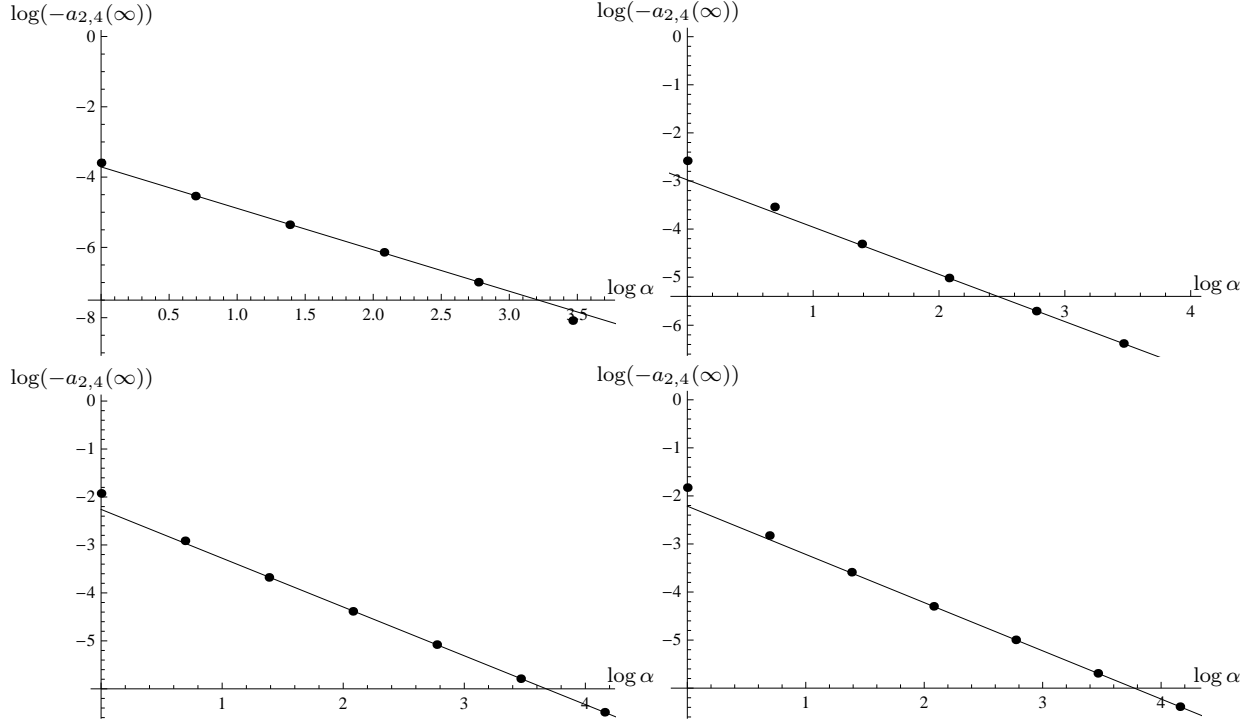


Figure 6: log-log plots for  $|a_{2,4}|$  versus  $\alpha$  for various  $\Delta$  in the slow quench regime. The fact that the plots tend to straight lines for positive values of  $\log \alpha$  means that  $a_{2,4}$  scales as a power law for large  $\alpha$ . Clockwise from the top left, the plots are for  $\Delta = 7/3, 8/3, 11/3$  and  $10/3$ .

### 9.3 Response for slow quenches

In figure 5, we plotted  $\phi_{(2\Delta-4)}$  as a function of  $\tau$  for the various values of  $\Delta$  and  $\alpha$ . The time is scaled by  $\alpha^{-1}$  so that the different plots would equilibrate in approximately the same distance on the horizontal axis. As  $\alpha$  grows large, the curves approach an inverted tanh graph, which is the expected adiabatic limit, *i.e.*,  $\phi_{(2\Delta-4)}(\infty)\phi_{(0)}(\tau)$  — see eq. (8.2). Note that in this case there is no need to rescale the vertical axis since  $\phi_{(2\Delta-4)}$  is of the same order in all cases.

As discussed in section 8,  $a_{2,4}(\infty)$ , which controls the entropy production, goes to zero in the adiabatic limit. Further, the analysis there showed that the leading contribution gave  $a_{2,4}(\infty) \propto 1/\alpha$  for slow quenches — see eq. (8.10). This behaviour is revealed in our numerical results in figure 6. There  $\log(-a_{2,4}(\infty))$  is shown as a function of  $\log \alpha$  and we see that for large  $\alpha$ , the results can be fit with a straight line

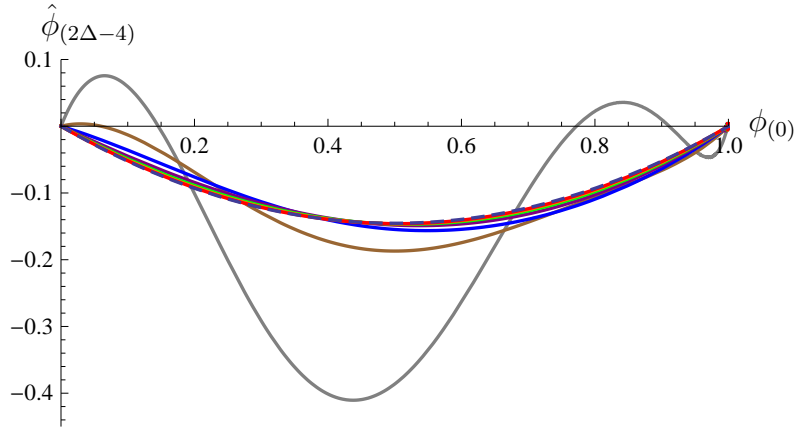


Figure 7: (Colour online) Plots of the deviation from the adiabatic response as a function of  $\phi_{(0)}$  for slow quenches with different speeds and  $\Delta = 11/3$  — see eq. (9.8) for the definition of  $\hat{\phi}_{(2\Delta-4)}$ . The curves correspond to  $\alpha = 1$  (grey), 2 (brown), 4 (blue), 8 (purple), 16 (green), 32 (orange) and 64 (red). The dashed curve corresponds to  $b_{(0)}\dot{\phi}_{(0)}$ .

with a slope of approximately  $-1$  in all the plots shown. Similar to the fast quench case, the straight lines are fit through the last three data-points in each plot.<sup>5</sup> Further the intercepts of the straight lines in figure 6 should correspond to (minus the logarithm of) the coefficients given in eq. (8.11). We defer the detailed comparison of the results derived in section 8 and with the numerical simulations here until section 10.

Again, although not shown, the same behaviour was also found for slow quenches in the case  $\Delta = 4$ . This behaviour was also found to hold for  $\Delta = 2$  and 3 in [12].

For slow quenches, let us define the deviation of the response from the adiabatic limit (8.2) as

$$\hat{\phi}_{(2\Delta-4)}(\tau) = \alpha \left( \phi_{(2\Delta-4)}(\tau) - \phi_{(2\Delta-4)}(\infty) \phi_{(0)}(\tau) \right). \quad (9.8)$$

As discussed in section 8, this function should be approximately given by  $b_{(0)}\dot{\phi}_{(0)}$ , where  $b_{(0)}$  was the coefficient of the normalizable mode in the radial profile of the  $1/\alpha$  contribution. Figure 7 shows the deviation  $\hat{\phi}_{(2\Delta-4)}$  as a function of  $\phi_{(0)}$  for  $\Delta = 11/3$  and different values of  $\alpha$ . The dashed curve shows  $b_{(0)}\dot{\phi}_{(0)}$ , where  $b_{(0)}$  was determined by the shooting method in section 8. As we can see in the figure, as  $\alpha$  grows large,

---

<sup>5</sup>Note that in the case  $\Delta = 7/3$  we fit the line through three intermediate points, since our result for  $a_{2,4}(\infty)$  contained a significant numerical error for the largest value of  $\alpha$  shown.

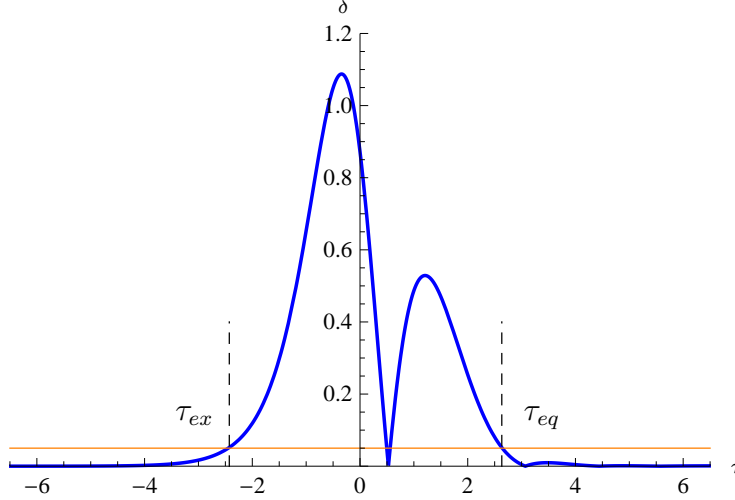


Figure 8: (Colour online) Plot of  $\delta$  as a function of  $\tau$  for  $\alpha = 1$  and  $\Delta = 8/3$ . The excitation time  $\tau_{ex}$  and relaxation time  $\tau_{eq}$  are shown as the first and final times, respectively, at which  $\delta$  crosses the threshold of  $\varepsilon = .05$  (shown as the orange line).

the deviation determined by our numerical simulations is converging on the expected curve. Those curves corresponding to larger  $\alpha$  fit the dashed curve best. The curve for  $\alpha = 64$  lies practically on top of the limiting dashed curve.

#### 9.4 Excitation and relaxation times

Next, we consider the excitation and relaxation times following the approach presented in [12]. First, we define

$$\delta \equiv \left| \frac{\phi_{(2\Delta-4)} - \phi_{(2\Delta-4)}(\infty)\phi_{(0)}}{\phi_{(2\Delta-4)}(\infty)} \right|, \quad (9.9)$$

*i.e.*, the absolute value of the relative deviation of the response  $\phi_{(2\Delta-4)}$  from the adiabatic limit  $\phi_{(2\Delta-4)}(\infty)\phi_{(0)}$ . Then we define the excitation time  $\tau_{ex}$  as the first time at which  $\delta$  reaches  $\varepsilon = .05$ , where the latter was chosen as an arbitrary threshold. Similarly, the relaxation or equilibration time  $\tau_{eq}$  is the latest time at which  $\delta$  drops below the  $\varepsilon = .05$  threshold. As an example,  $\delta$  is shown in figure 8 for  $\alpha = 1$  and  $\Delta = 8/3$ . The vertical grid lines indicate the excitation time  $\tau_{ex}$  and relaxation time  $\tau_{eq}$ . Note that our definitions of  $\tau_{ex}$  and  $\tau_{eq}$  is only expected to be meaningful for relatively small  $\alpha$ . As  $\alpha$  grows large, the response approaches the adiabatic profile (8.2) and so for sufficiently large  $\alpha$ ,  $\delta$  will never exceed the chosen threshold.

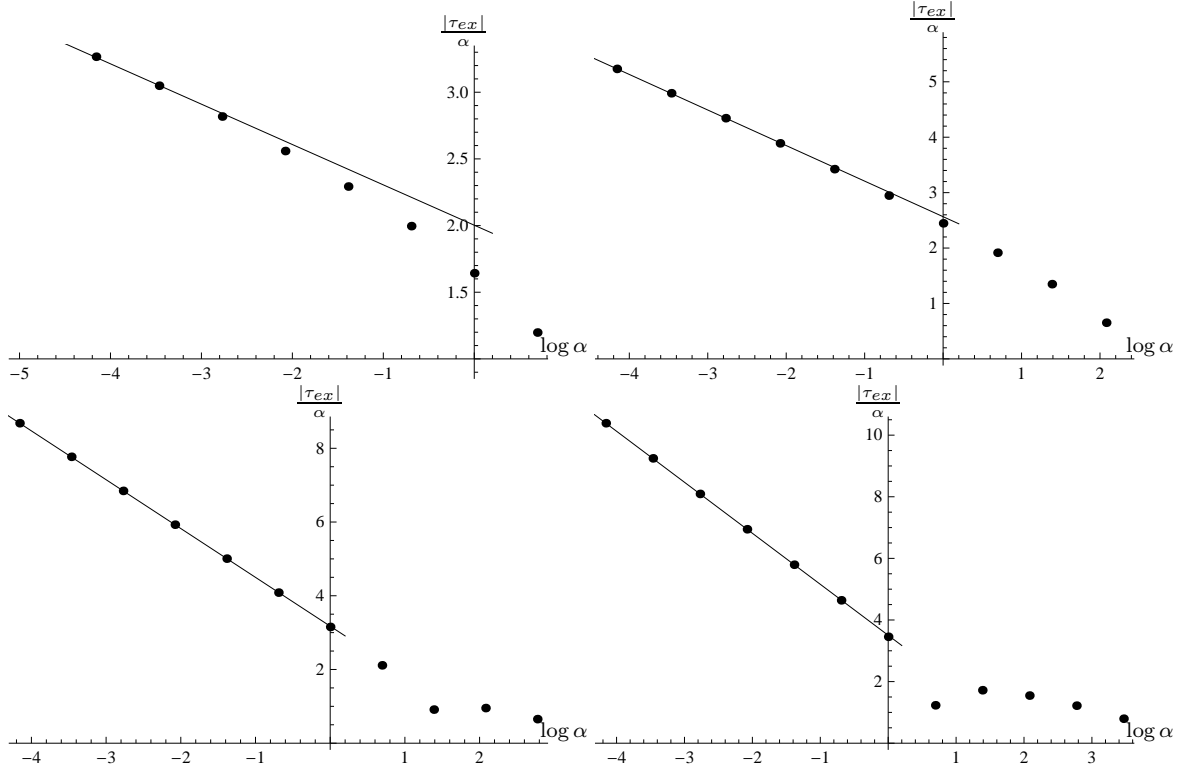


Figure 9: Plots of  $\frac{|\tau_{ex}|}{\alpha}$  as a function of  $\log \alpha$ . The straight lines indicate the asymptotic behaviour for fast quenches. Clockwise from the top left, the plots are for  $\Delta = 7/3$ ,  $8/3$ ,  $11/3$  and  $10/3$ .

Figure 9 shows the rescaled excitation time  $|\tau_{ex}|/\alpha$  as a function of  $\log \alpha$  for different values of  $\Delta$ . For fast quenches (*i.e.*,  $\log \alpha \leq 0$ ), we see that  $|\tau_{ex}|/\alpha$  approaches a straight line, indicating that the excitation time scales as  $\beta_{\Delta} \alpha \log \alpha$ . Once again the straight lines are fit through the three points with the points corresponding to the fastest quenches, for each  $\Delta$ . The constants  $\beta_{\Delta}$  can be determined as the slope of the fitted line in these plots. The plots also show that, as expected, the behaviour becomes irregular for  $\log \alpha > 0$ , in particular for  $\Delta = 10/3$  and  $11/3$ .

Figure 10 shows the slopes of the straight-line fits in the previous plots as a function of  $\Delta$ . This plot also includes data-points for  $\Delta = 2$  and  $3$  using the results in [12].<sup>6</sup> The fact that  $\frac{\partial |\tau_{ex}|/\alpha}{\partial \log \alpha} = 0$  for  $\Delta = 2$  means that in this case  $\tau_{ex}$  has no  $\log \alpha$ -dependence

---

<sup>6</sup>For these two points, we have used the expressions for  $|\tau_{ex}|/\alpha$  after the  $\log(-\log \alpha)$  terms have been subtracted.

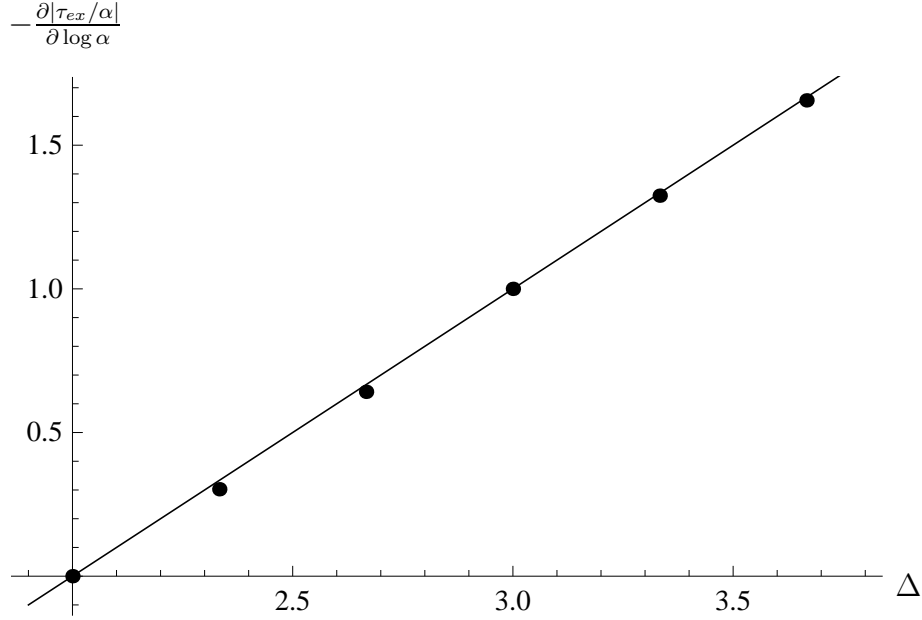


Figure 10: A plot of (minus) the slope of the fitted straight lines in figure 9. The datapoints lie approximately on the predicted line  $-\frac{\partial|\tau_{ex}/\alpha|}{\partial \log \alpha} = \Delta - 2$  shown. Also shown are the data for  $\Delta = 2$  and 3 from [12].

for this type of quench. We find that the datapoints lie approximately on the line

$$-\frac{\partial|\tau_{ex}|/\alpha}{\partial \log \alpha} = \Delta - 2, \quad (9.10)$$

which is numerically almost identical to the fitted line through all the data-points shown in the figure, namely

$$-\frac{\partial|\tau_{ex}|/\alpha}{\partial \log \alpha} = 1.003\Delta - 2.02. \quad (9.11)$$

Hence for fast quenches, *i.e.*,  $\alpha \ll 1$ , the excitation time scales as

$$\tau_{ex} \simeq (\Delta - 2) \alpha \log \alpha. \quad (9.12)$$

Using the same approach, we also studied the relaxation time  $\tau_{eq}$ . In this case for all of the various  $\Delta$ , we found

$$\tau_{eq} \approx \alpha^0, \quad (9.13)$$

for fast quenches. That is,  $\tau_{eq}$  is constant for small  $\alpha$ , rather than scaling with  $\alpha$  in some way, for all (fractional)  $\Delta$ . This behaviour is consistent with the results for  $\Delta = 2$



and 3, found in [12]. In terms of the dimensionful time coordinate  $t$ , the relaxation time is  $t_{eq} \sim 1/\mu$ . In terms of the boundary theory then, the relaxation time is set by the thermal timescale for fast quenches.

## 9.5 Behaviour of the energy and pressure

Recall that our analysis was restricted to considering conformal dimensions in the range  $2 < \Delta < 4$ . With this restriction, the change in the temperature  $\Delta T$  and energy density  $\Delta \mathcal{E}$  will always be positive in our holographic quenches, as is evident from eqs. (6.25) and (6.26). On the other hand, eqs. (6.35) and (6.36) show that  $\Delta T$  and  $\Delta \mathcal{E}$  may have either sign for the reverse quenches considered in section 6.3. In particular, in the adiabatic limit,  $\tilde{a}_{2,4}(\infty)$  vanishes and so we have both  $\Delta T < 0$  and  $\Delta \mathcal{E} < 0$ . Then as  $\alpha$  becomes smaller,  $\tilde{a}_{2,4}(\infty)$  grows and eventually  $\Delta T$  and  $\Delta \mathcal{E}$  become positive. Specifically, eqs. (6.35) and (6.36) indicate:

$$\Delta T > 0 \quad \text{for} \quad |\tilde{a}_{2,4}(\infty)| > \frac{2}{3} (\Delta - 2)^2 |\tilde{\phi}_{(2\Delta-4)}(-\infty)|, \quad (9.14)$$

$$\Delta \mathcal{E} > 0 \quad \text{for} \quad |\tilde{a}_{2,4}(\infty)| > \frac{1}{3} (\Delta - 2) |\tilde{\phi}_{(2\Delta-4)}(-\infty)|. \quad (9.15)$$

Recall that  $\tilde{\phi}_{(2\Delta-4)}(-\infty) = \phi_{(2\Delta-4)}(\infty)$  corresponds to the equilibrium response given in eq. (6.13). With our numerical simulations, we determined the value of  $\alpha$  at which these thresholds are reached for various values of  $\Delta$  and the results are shown in table 2. We have also included the analogous results for  $\Delta = 2$  and 3 from [12]. Note the qualitative trend is that the threshold value of  $\alpha$  grows monotonically as  $\Delta$  increases. Note that eqs. (9.14) and (9.15) imply that the threshold for positive  $\Delta \mathcal{E}$  is greater than that for positive  $\Delta T$  (*i.e.*, larger  $\alpha$ ) for  $\Delta > 2.5$ , while the thresholds are reversed for  $\Delta < 2.5$ . Clearly, this behaviour is reflected in the results shown in table 2.

Turning now to the change in the pressure  $\Delta \mathcal{P}$ , we have eqs. (6.27) and (6.37) for forward and reverse quenches, respectively. In this case,  $\Delta \mathcal{P} > 0$  in all forward quenches as long as  $\Delta > 7/2$  and in all reverse quenches for  $\Delta < 7/2$ . Otherwise, the sign of  $\Delta \mathcal{P}$  will depend on the rate of the quench. Here we focus on the forward quenches with  $\Delta < 7/2$ . In this case,  $\Delta \mathcal{P} < 0$  for slow quenches and as  $\alpha$  decreases, the change in the pressure reverses its sign when

$$\Delta \mathcal{P} > 0 \quad \text{for} \quad |a_{2,4}(\infty)| > \frac{1}{3} (7 - 2\Delta) (\Delta - 2) |\phi_{(2\Delta-4)}(\infty)|. \quad (9.16)$$

The value of  $\alpha$  at which these thresholds is reached for various values of  $\Delta$  is shown in table 2. Again, we have also included an analogous result for  $\Delta = 3$  [12]. The

Table 2: Approximate upper bounds on  $\alpha$  for which  $\Delta T > 0$  and  $\Delta \mathcal{E} > 0$  for reverse quenches. The upper bounds on  $\alpha$  for  $\Delta \mathcal{P} > 0$  is for forward quenches when  $\Delta < 3.5$ , with different values of  $\Delta$ . For  $\Delta = 2$  the values of  $\Delta \mathcal{E}$  and  $\Delta \mathcal{P}$  are renormalization scheme dependent, see [12].

$\Delta$	$\Delta T$	$\Delta \mathcal{E}$	$\Delta \mathcal{P}$
2	0.58		
7/3	0.68	0.50	0.23
8/3	0.77	0.92	0.68
3	0.86	1.32	1.32
10/3	1.00	2.00	5.5
11/3	1.41	4.00	–

qualitative trend is that the threshold value of  $\alpha$  grows monotonically as  $\Delta$  increases. Further, we may compare the above threshold to those in eqs. (9.14) and (9.15).<sup>7</sup> In particular, the threshold for positive  $\Delta \mathcal{P}$  is greater than that for positive  $\Delta \mathcal{E}$  for  $\Delta > 3$ , while the thresholds are reversed for  $\Delta < 3$ . We also find the threshold for positive  $\Delta \mathcal{P}$  is less than that for positive  $\Delta T$  when  $\Delta < 2.75$ . Clearly, this behaviour is reflected in the results shown in table 2.

## 10 Discussion

In this paper, we continued the program initiated in [12] of studying quantum quenches in strongly coupled quantum field theories using holography. The process studied here was the quench of a four-dimensional conformal field theory made with a rapid transition in the coupling of a relevant operator  $\mathcal{O}_\Delta$  from zero to some finite value  $\lambda_f$ . Ref. [12] had considered the special cases where the conformal dimension of the operator was  $\Delta = 2$  and 3. Our holographic analysis allowed for operators with general conformal dimensions in the range  $2 < \Delta < 4$ . Through the gauge/gravity correspondence [5], this quench was translated to a classical problem in five-dimensional Einstein gravity coupled to a negative cosmological constant and a (free) massive scalar field.

---

<sup>7</sup>Note that here we are comparing a threshold for the forward quenches to thresholds in the reverse quenches.

In particular, the quench was implemented by introducing a time-dependent boundary condition on the scalar field in the asymptotically AdS<sub>5</sub> spacetime. Our discussion also only considered quenches of a thermal plasma with an initial temperature  $T_i$  in the boundary theory and was limited to a high temperature regime<sup>8</sup> where  $\lambda_f \ll T_f^{4-\Delta}$ . Hence our calculations were perturbative in the ratio  $\lambda_f/T_f^{4-\Delta}$ , which in the gravitational description meant that they were perturbative in the (dimensionless) amplitude of the bulk scalar. However, there was no restriction on the timescale  $\Delta t$  governing the transition rate of the coupling. In particular, with the transition profiles in eq. (7.1), our results were described in terms of the dimensionless parameter:  $\alpha = \pi T_i \Delta t$ , *i.e.*, the ratio of the transition timescale to the relaxation timescale of the thermal plasma. In our analysis, we paid special attention to the limit of adiabatic transitions with  $\alpha \rightarrow \infty$  and of very fast quenches with  $\alpha \rightarrow 0$ . A detailed discussion of the results was given in section 9.

In all of these quenches, our computations implicitly gave the response in the one-point correlators of the relevant operator  $\langle \mathcal{O}_\Delta \rangle$  and the stress tensor  $\langle T_{ij} \rangle$ , as described by eqs. (5.4)–(5.6), to leading order in  $\lambda_f/T_f^{4-\Delta}$ . In section 9, our discussion of the results was presented in terms of two gravitational parameters,  $\phi_{2\Delta-4}(\tau)$  and  $a_{2,4}(\infty)$ . With eq. (5.6), we see the first is directly related to  $\langle \mathcal{O}_\Delta \rangle$  during the quench. We can rewrite this expression as

$$\langle \mathcal{O}_\Delta \rangle = \frac{\pi^4 C_T}{40} (\Delta - 2) \frac{\lambda_f}{T_f^{4-2\Delta}} \frac{\phi_{2\Delta-4}(t/\pi T_f)}{|\phi_{2\Delta-4}(\infty)|}, \quad (10.1)$$

using eq. (2.5) and various results from section 6. Further  $a_{2,4}(\infty)$  controls the entropy production (6.24), as well as the changes in the temperature, energy and pressure as given in eqs. (6.25)–(6.27). One confirmation of our numerical simulations was that we found  $a_{2,4}(\infty) \leq 0$  for all of our quenches with any values of  $\alpha$  and  $\Delta$ . With eq. (6.24), the latter ensures that the entropy production was always positive, in accord with the second law of thermodynamics.

Another confirmation comes from our analysis of slow quenches in section 8. In this case with  $\alpha \gg 1$ , it was shown that the linearized equation (3.5) for the bulk scalar can be solved using a power series in  $1/\alpha$ . While  $a_{2,4}(\infty)$  vanishes for the leading adiabatic solution, we showed that a  $1/\alpha$  contribution appears at the next order in eq. (8.10). Using a shooting method, we explicitly solved for this contribution and the results were given in eq. (8.11). This same leading order contribution to  $a_{2,4}(\infty)$  for

---

<sup>8</sup>In fact, this inequality is satisfied by the coupling and temperature throughout the quench.

slow quenches is addressed with the numerical results shown in figure 6. In these plots, the same approximate  $1/\alpha$  scaling was found with an asymptotic straight-line fit in  $\log \alpha$  for  $\alpha \gg 1$ , *i.e.*,

$$\log |a_{2,4}(\infty)| = -c - \log \alpha. \quad (10.2)$$

The case  $\Delta = 7/3$  had the worst fit, with a slope differing from  $-1$  by about 18%. We believe that the slow convergence in our numerical simulations for this case led to this relatively large error. The other three cases in table 3 had slopes that differed from the expected slope by 2% or less. As well as obtaining a fair match in the slope above, we can compare the intercept  $c$  coming from these numerical results with that calculated from the independently derived results in eq. (8.11). We see in table 3 that the intercepts derived from the two approaches agree very well. Recall that in figure 7, we also showed that the full time-dependent profile of the numerical response (after subtracting the adiabatic profile) matched well with the form derived in section 8 for  $\alpha \gg 1$ .

Table 3: Intercept in eq. (10.2) evaluated by two different methods:  $c_{shoot}$  is derived from the results in eq. (8.11), while  $c_{numer}$  comes from fitting the data in figure 6.

$\Delta$	$c_{shoot}$	$c_{numer}$	$\frac{c_{shoot} - c_{numer}}{c_{shoot}}$
7/3	3.93	3.71	5.6%
8/3	2.96	2.98	-0.68%
10/3	2.31	2.26	2.2%
11/3	2.22	2.21	0.45%

In eq. (9.12), we found an interesting scaling behaviour for the excitation time in fast quenches, namely  $\tau_{ex} \simeq (\Delta - 2)\alpha \log \alpha$ . On the one hand, this indicates that the excitation time is longer when the conformal dimension of the operator is larger but it also shows that  $\tau_{ex}$  becomes shorter for faster quenches. In particular,  $\tau_{ex} \rightarrow 0$  for  $\alpha \rightarrow 0$ , for which the quench profile (7.1) becomes a step-function at  $\tau = 0$ . In contrast, as shown in eq. (9.13), the relaxation time remains constant for  $\alpha \ll 1$ . Hence independent of the precise values of  $\Delta$  and  $\alpha$ , the boundary system relaxes on the thermal timescale  $1/T$  for fast quenches.

Perhaps, the most interesting result coming from our analysis was the universal behaviour found in  $|\phi_{2\Delta-4}|$  and  $a_{2,4}(\infty)$  for  $\alpha \ll 1$ . Of course, in terms of the boundary

theory, these results translate into universal behaviour in the response of  $\langle \mathcal{O}_\Delta \rangle$  and in the thermodynamic quantities for fast quenches. First, the results in figure 1 indicate that the maximum value of  $|\phi_{2\Delta-4}|$  scales as  $\alpha^{-(2\Delta-4)}$ , which with eq. (10.1), translates into a scaling for the expectation value of the quenched operator, *i.e.*,

$$\max \langle \mathcal{O}_\Delta \rangle \propto \frac{1}{\alpha^{2\Delta-4}}. \quad (10.3)$$

Beyond this scaling, figure 2 also indicates that the response and hence  $\langle \mathcal{O}_\Delta \rangle$  approach a relatively simple universal form in the limit  $\alpha \rightarrow 0$ . These results are in agreement with those found previously in [12]. However, we might comment that our analysis here assumed that  $\Delta$  was a fraction, whereas [12] studied the special cases  $\Delta = 2$  and  $3$ . In both of these cases, the response also exhibited an additional contribution which scaled faster than shown in eq. (10.3) by an extra logarithmic factor. An extra logarithmic factor is also present for  $\Delta = 4$  [31].

The above scaling of  $|\phi_{2\Delta-4}|$  also leads to the scaling of  $a_{2,4}(\infty) \propto \alpha^{-(2\Delta-4)}$  for fast quenches, as shown with the numerical data in figure 4. This contribution then dominates in eqs. (6.24)–(6.27) and so the changes of the various thermodynamic quantities induced by fast quenches exhibit the same scaling, *e.g.*,

$$\frac{\Delta \mathcal{E}}{\mathcal{E}_i} \propto \frac{1}{\alpha^{2\Delta-4}} \quad (10.4)$$

for  $\alpha \ll 1$ . Again these results are in agreement with those found in [12]. However, the results there and in [31] indicate that eq. (10.4) is further enhanced by a logarithmic scaling for  $\Delta = 2$ . While quenches by operators with conformal dimensions in the range  $2 \leq \Delta \leq 4$  are covered by the analysis here and in [12], it would be interesting to understand if this universal behaviour extends to the allowed regime  $1 \leq \Delta < 2$ . We will consider this possibility in a later paper [31].

As noted in [12], given the scaling in eqs. (10.3) and (10.4), it appears that ‘infinitely fast’ quenches seem to be ill-defined because physical quantities are diverging as  $\alpha \rightarrow 0$ . Recall that in this limit, the quench profile (7.1) becomes a step-function at  $\tau = 0$ . Hence this issue is particularly notable since it is precisely such ‘infinitely fast’ quenches are studied in the seminal work on this topic [3]. However, we must contrast their description of a quench with the present approach. In [3], the system is evolved from  $t = -\infty$  to  $0^-$  to prepare the system in a far-from-equilibrium state of the ‘quenched’ Hamiltonian, *i.e.*, the ground state of the initial Hamiltonian. This state is then used as the initial condition at  $t = 0^+$  and the subsequent evolution of the system with the ‘quenched’ Hamiltonian is studied.

Of course, since the present calculations are only perturbative in  $\lambda_f/T_f^{4-\Delta}$ , one can not take the singularities appearing in eqs. (10.3) and (10.4) for  $\alpha \rightarrow 0$  too seriously. Hence it would be interesting to study the fast quenches by evolving the full nonlinear equations of the dual gravity theory. At present, our preliminary analysis suggests that in fact these singularities are physical [31]. In any event, the present holographic calculations illustrate that the gauge/gravity correspondence provides a versatile new framework for the study of quantum quenches. Undoubtedly, interesting new lessons will come from applying holography to study more general physical quantities and the behaviour of more complicated systems under a quench. This will help build our intuition for the behaviour of fast-changing quantum fields that occur when the external parameters are changed in laboratory experiments.

## Acknowledgments

AvN would like to thank Ross Diener and Alex Yale for helpful discussions. Research at Perimeter Institute is supported by the Government of Canada through Industry Canada and by the Province of Ontario through the Ministry of Research & Innovation. AB, LL and RCM gratefully acknowledge support from NSERC Discovery grants. Research by LL and RCM is further supported by funding from the Canadian Institute for Advanced Research.

## A Coefficients in the metric solution

Here we list the expressions of the coefficients in the metric functions (3.11) and (3.12) in terms of the normalizable and non-normalizable modes of the scalar,  $\phi_{(0)}$  and  $\phi_{(2\Delta-4)}$ . We only list the coefficients that are needed (and the first subleading coefficient) in calculating the boundary stress tensor and the expectation value of the operator  $\mathcal{O}_\Delta$ .

Because  $\dot{a}_{2,4}$  depends on it, we will give the expression for  $a_{2,5}$ , even though it is subleading and has only vanishing contributions to physical quantities:

$$a_{2,5} = \frac{1}{18} \left( \Delta(2\Delta - 5) \dot{\phi}_{(0)} \phi_{(2\Delta-2)} - (2\Delta - 3)(4 - \Delta) \phi_{(0)} \dot{\phi}_{(2\Delta-2)} \right). \quad (\text{A.1})$$

The coefficients of the terms with negative powers of  $2\Delta$  in  $A_p$  are given by

$$\alpha_{2,4} = -\frac{(4-\Delta)\phi_{(0)}^2}{6(7-2\Delta)}; \quad (\text{A.2})$$

$$\alpha_{2,5} = \frac{(\Delta-3)\phi_{(0)}\dot{\phi}_{(0)}}{3(7-2\Delta)}; \quad (\text{A.3})$$

$$\alpha_{2,6} = \frac{(2\Delta^2-6\Delta+15)\dot{\phi}_{(0)}^2 + (2\Delta^2-13\Delta+24)\phi_{(0)}\ddot{\phi}_{(0)}}{12(\Delta-3)(9-2\Delta)}; \quad (\text{A.4})$$

$$\alpha_{2,7} = \frac{(4-\Delta)\left(-3(\Delta-2)(9-2\Delta)\dot{\phi}_{(0)}\ddot{\phi}_{(0)} + (2\Delta^2-15\Delta+36)\phi_{(0)}\ddot{\phi}_{(0)}\right)}{36(5-\Delta)(\Delta-3)(9-2\Delta)} \quad (\text{A.5})$$

$$\begin{aligned} \alpha_{2,8} = & -\left(12(5-\Delta)(4-\Delta)^2(\Delta-3)^2(2\Delta^2-11\Delta+30)\phi_{(0)}^2\right. \\ & -3(7-2\Delta)^2(5-\Delta)(2\Delta^3-19\Delta^2+56\Delta-54)\ddot{\phi}_{(0)}^2 \\ & -4(\Delta-3)(7-2\Delta)(2\Delta^2-14\Delta+21)(2\Delta^2-17\Delta+39)\dot{\phi}_{(0)}\phi_{(0)}^{(3)} \\ & \left.+ (4-\Delta)(\Delta-3)(9-2\Delta)(2\Delta-7)(2\Delta^2-17\Delta+51)\phi_{(0)}\phi_{(0)}^{(4)}\right) \\ & \left/ (288(5-\Delta)(4-\Delta)(\Delta-3)^2(4\Delta^2-36\Delta+77))\right). \end{aligned} \quad (\text{A.6})$$

Of the coefficients to the terms with positive of powers  $2\Delta$  in  $A_p$ , the coefficient

$$\beta_{2,4} = \frac{\Delta\phi_{(2\Delta-2)}^2}{6(2\Delta-1)} \quad (\text{A.7})$$

will be subleading.

The coefficients in  $\Sigma_p$  corresponding to integer powers of  $\rho$  are given by

$$s_{2,5} = -\frac{\Delta(4-\Delta)\phi_{(0)}\phi_{(2\Delta-4)}}{36}; \quad (\text{A.8})$$

$$s_{2,6} = -\frac{1}{60}\left(\Delta(5-\Delta)\dot{\phi}_{(0)}\phi_{(2\Delta-4)} + (4-\Delta)(\Delta+1)\phi_{(0)}\dot{\phi}_{(2\Delta-4)}\right). \quad (\text{A.9})$$

The coefficients of the terms with negative powers of  $2\Delta$  in  $\Sigma_p$  are given by

$$\sigma_{2,5} = -\frac{(4-\Delta)\phi_{(0)}^2}{12(7-2\Delta)}; \quad (\text{A.10})$$

$$\sigma_{2,6} = -\frac{(5-\Delta)\phi_{(0)}\dot{\phi}_{(0)}}{6(9-2\Delta)}; \quad (\text{A.11})$$

$$\sigma_{2,7} = \frac{2(5-\Delta)^2(\Delta-3)\dot{\phi}_{(0)}^2 + (6-\Delta)(4-\Delta)(7-2\Delta)\phi_{(0)}\ddot{\phi}_{(0)}}{24(5-\Delta)(\Delta-3)(9-2\Delta)}; \quad (\text{A.12})$$

$$\begin{aligned} \sigma_{2,8} = & \frac{3(6-\Delta)(5-\Delta)(7-2\Delta)\dot{\phi}_{(0)}\ddot{\phi}_{(0)}}{72(5-\Delta)(\Delta-3)(11-2\Delta)} \\ & + \frac{(7-\Delta)(4-\Delta)(9-2\Delta)\phi_{(0)}\phi_{(0)}^{(3)}}{72(5-\Delta)(\Delta-3)(11-2\Delta)}; \end{aligned} \quad (\text{A.13})$$

$$\begin{aligned} \sigma_{2,9} = & -\left(12(8-\Delta)(4-\Delta)^2(\Delta-3)^2\phi_{(0)}^2 - 3(7-2\Delta)^2(6-\Delta)^2\ddot{\phi}_{(0)}^2\right. \\ & - 8(7-\Delta)(5-\Delta)(\Delta-3)(9-2\Delta)\dot{\phi}_{(0)}\phi_{(0)}^{(3)} \\ & \left. - (8-\Delta)(\Delta-3)(11-2\Delta)(9-2\Delta)\phi_{(0)}\phi_{(0)}^{(4)}\right) \\ & / \left(576(6-\Delta)(\Delta-3)^2(11-2\Delta)\right). \end{aligned} \quad (\text{A.14})$$

Of the coefficients to the terms with positive of powers  $2\Delta$  in  $\Sigma_p$ , the coefficient

$$\theta_{2,5} = \frac{\Delta\phi_{(2\Delta-2)}^2}{12(2\Delta-1)} \quad (\text{A.15})$$

is subleading.

## B Coefficients in the Fefferman-Graham coordinates

### B.1 The time and radial coordinates

The expansion of the EF time and radial coordinates in terms of the FG time and radial coordinates was given in eqs. (4.5) and (4.6). The expressions of the coefficients can be written in terms of the coefficients  $\phi_{(0)}$ ,  $\phi_{(2\Delta-4)}$  and  $a_{2,4}$ . First, the terms containing  $v_n$  and  $\rho_n$  are given by the series

$$\sum_n v_n r^n = -r - \frac{3r^5\mu^4}{40} - \frac{11r^9\mu^8}{1152} - \frac{23r^{13}\mu^{12}}{13312} + \dots, \quad (\text{B.1})$$

$$\sum_n \rho_n r^n = -\frac{r^5\mu^5}{8} + \frac{3r^9\mu^9}{128} - \frac{5r^{13}\mu^{13}}{1024} + \dots \quad (\text{B.2})$$



Next, the terms of order  $\ell^2$  are given by

$$\sum_{n=5} \vartheta_n r^n = \frac{3}{40} r^5 \mu^4 a_{2,4} + \frac{1}{240} r^6 \mu^4 (16\mu a_{2,5} - 11\partial_t a_{2,4}) + \dots, \quad (\text{B.3})$$

$$\sum_{n=5} \chi_n r^n = \frac{1}{8} r^5 \mu^5 a_{2,4} + \frac{1}{10} r^6 \mu^5 (\mu a_{2,5} - \partial_t a_{2,4}) + \dots, \quad (\text{B.4})$$

where the terms of order  $r^6$  only make subleading contributions in the calculated quantities. The coefficients of the terms with factors of  $r^{-2\Delta}$  in  $\tau/\mu$  are given by

$$\begin{aligned} \nu_0 &= \frac{(7-2\Delta)\mu^{2\Delta-8}\alpha_{2,4}}{4(4-\Delta)(9-2\Delta)}; \\ \nu_1 &= \frac{\mu^{8-2\Delta}((4\Delta^2-30\Delta+55)\partial_t\alpha_{2,4}+4(4-\Delta)^2\mu\alpha_{2,5})}{8(5-\Delta)(11-\Delta)(9-2\Delta)}; \\ \nu_2 &= \mu^{8-2\Delta} \frac{(4\Delta^2-32\Delta+61)\partial_t^2\alpha_{2,4}}{8(5-\Delta)(11-2\Delta)(9-2\Delta)} \\ &\quad + \mu^{8-2\Delta} \frac{-2(4\Delta^2-34\Delta+71)\mu\partial_t\alpha_{2,5}+2(9-2\Delta)^2\mu^2\alpha_{2,6}}{8(5-\Delta)(11-2\Delta)(9-2\Delta)}; \\ \nu_3 &= -\mu^{8-2\Delta} \frac{(4\Delta^2-34\Delta+67)\partial_t^3\alpha_{2,4}-6(2\Delta^2-18\Delta+39)\mu\partial_t^2\alpha_{2,5}}{48(6-\Delta)(5-\Delta)(11-2\Delta)} \\ &\quad - \mu^{8-2\Delta} \frac{6(4\Delta^2-38\Delta+89)\mu^2\partial_t\alpha_{2,6}-24(5-\Delta)^2\mu^3\alpha_{2,7}}{48(6-\Delta)(5-\Delta)(11-2\Delta)}, \end{aligned} \quad (\text{B.5})$$

where  $\alpha_{2,n}$  are the coefficients defined in eq. (3.11) and given explicitly in eqs. (A.2)–(A.5) — implicitly, functions of the FG time  $t$  here. Similarly, the coefficients in  $\rho$  with factors of  $r^{-2\Delta}$  are given by

$$\xi_0 = \frac{\mu^{9-2\Delta}\alpha_{2,4}}{4(4-\Delta)}; \quad (\text{B.6})$$

$$\xi_1 = -\frac{\mu^{9-2\Delta}(\partial_t\alpha_{2,4}-\mu\alpha_{2,5})}{2(9-2\Delta)}; \quad (\text{B.7})$$

$$\xi_2 = \frac{\mu^{9-2\Delta}(\partial_t^2\alpha_{2,4}-2\mu\partial_t\alpha_{2,5}+2\mu^2\alpha_{2,6})}{8(5-\Delta)}; \quad (\text{B.8})$$

$$\xi_3 = -\frac{\mu^{9-2\Delta}(\partial_t^3\alpha_{2,4}-3\mu\partial_t^2\alpha_{2,5}+6\mu^2\partial_t\alpha_{2,6}-6\mu^3\alpha_{2,7})}{12(11-2\Delta)}; \quad (\text{B.9})$$

$$\begin{aligned} \xi_4 &= -\frac{\mu^{9-2\Delta}((2\Delta^2-13\Delta+30)\mu^4\alpha_{2,4}-(4-\Delta)\partial_t^5\alpha_{2,4})}{32(6-\Delta)(4-\Delta)} \\ &\quad - \frac{\mu^{9-2\Delta}(4\mu\partial_t^3\alpha_{2,5}-12\mu^2\partial_t^2\alpha_{2,6}+24\mu^3\partial_t\alpha_{2,7}-24\mu^4\alpha_{2,8})}{96(6-\Delta)}. \end{aligned} \quad (\text{B.10})$$

The coefficients of the terms with factors of  $r^{2\Delta}$  in  $v$  are given by

$$\omega_1 = \frac{(2\Delta - 1)\mu^{2\Delta}\beta_{2,4}}{4\Delta(2\Delta + 1)}; \quad (\text{B.11})$$

$$\omega_2 = -\frac{\mu^{2\Delta}((4\Delta^2 - 2\Delta - 1)\partial_t\beta_{2,4} - 4\Delta^2\mu\beta_{2,5})}{8\Delta(\Delta + 1)(2\Delta + 1)}; \quad (\text{B.12})$$

$$\begin{aligned} \omega_3 = & \mu^{2\Delta} \frac{(4\Delta^2 - 3)\partial_t^2\beta_{2,4}}{8(4\Delta^3 + 12\Delta^2 + 11\Delta + 3)} \\ & - \mu^{2\Delta} \frac{2(4\Delta^2 + 2\Delta - 1)\mu\partial_t\beta_{2,5} - 2(2\Delta + 1)^2\mu^2\beta_{2,6}}{8(4\Delta^3 + 12\Delta^2 + 11\Delta + 3)}; \end{aligned} \quad (\text{B.13})$$

$$\begin{aligned} \omega_4 = & -\mu^{2\Delta} \frac{(4\Delta^2 + 2\Delta - 5)\partial_t^3\beta_{2,4} - 6(2\Delta^2 + 2\Delta - 1)\mu\partial_t^2\beta_{2,5}}{48(\Delta + 1)(\Delta + 2)(2\Delta + 3)} \\ & - \mu^{2\Delta} \frac{(4\Delta^2 + 6\Delta + 1)\mu^2\partial_t\beta_{2,6} - 4(\Delta + 1)^2\mu^3\beta_{2,7}}{12(\Delta + 1)(\Delta + 2)(2\Delta + 3)}, \end{aligned} \quad (\text{B.14})$$

where  $\beta_{2,n}$  are the coefficients defined in eq. (3.11) — implicitly, functions of the FG time  $t$  here. Similarly, the coefficients in  $\rho$  with factors of  $r^{2\Delta}$  are given by

$$\zeta_1 = \frac{\mu^{2\Delta+1}\beta_{2,4}}{4\Delta}; \quad (\text{B.15})$$

$$\zeta_2 = -\frac{\mu^{2\Delta+1}(\partial_t\beta_{2,4} - \mu\beta_{2,5})}{2(2\Delta + 1)}; \quad (\text{B.16})$$

$$\zeta_3 = \frac{\mu^{2\Delta+1}(\partial_t^2\beta_{2,4} - 2\mu\partial_t\beta_{2,5} + 2\mu^2\beta_{2,6})}{8(\Delta + 1)}; \quad (\text{B.17})$$

$$\zeta_4 = -\frac{\mu^{2\Delta+1}(\partial_t^3\beta_{2,4} - 3\mu\partial_t^2\beta_{2,5} + 6\mu^2\partial_t\beta_{2,6} - 6\mu^3\beta_{2,7})}{12(2\Delta + 3)}; \quad (\text{B.18})$$

$$\begin{aligned} \zeta_5 = & -\mu^{2\Delta+1} \frac{3(2\Delta^2 - 3\Delta + 10)\mu^4\beta_{2,4} - \Delta\partial_t^4\beta_{2,4}}{96\Delta(\Delta + 2)} \\ & - \mu^{2\Delta+1} \frac{\Delta(4\mu\partial_t^3\beta_{2,5} - 12\mu^2\partial_t^2\beta_{2,6} + 24\mu^3\partial_t\beta_{2,7} - 24\mu^4\beta_{2,8})}{96\Delta(\Delta + 2)}. \end{aligned} \quad (\text{B.19})$$

## B.2 The metric

The expansion of the metric in the FG coordinates was given in eq. (2.8). The nonzero components for our purposes are the parts  $G_{00}$ , which correspond to the EF metric function  $-A$ , and the diagonal components of  $G_{ij}$ , which correspond to  $\Sigma^2$ . The order  $\ell^0$  terms in the metric are given by

$$g_{00}^{(0)} + r^4 g_{00}^{(4)} = -1 + \frac{3r^4\mu^4}{4} + o(r^8), \quad (\text{B.20})$$

$$g_{ii}^{(0)} + r^4 g_{ii}^{(4)} = 1 + \frac{\mu^4 r^4}{4} + o(r^8), \quad (\text{B.21})$$

where in the second line, we are indicating the three individual diagonal components, *i.e.*, there is no implicit sum over  $i$ . Next we list the terms of order  $\ell^2$ :

$$c_{(4)00} = -\frac{3}{4}\mu^4 a_{2,4}, \quad (\text{B.22})$$

$$c_{(4)ii} = -\frac{\mu^4}{4} \left( a_{2,4} + \frac{2}{9}\Delta(4-\Delta) \phi_{(0)}\phi_{(2\Delta-4)} \right). \quad (\text{B.23})$$

The coefficients of the terms with factors of  $r^{-2\Delta}$  in  $G_{00}$  are given by

$$d_{(0)00} = -\frac{(7-2\Delta)\mu^{8-2\Delta}\alpha_{2,4}}{2(4-\Delta)}; \quad (\text{B.24})$$

$$d_{(1)00} = -2\mu^{8-2\Delta} \frac{(\Delta-3)\partial_t\alpha_{2,4} + (4-\Delta)\mu\alpha_{2,5}}{9-2\Delta}; \quad (\text{B.25})$$

$$\begin{aligned} d_{(2)00} = & \mu^{8-2\Delta} \frac{(\Delta-3)(7-2\Delta)\partial_t^2\alpha_{2,4}}{4(5-\Delta)(4-\Delta)} \\ & + \mu^{8-2\Delta} \frac{2(7-2\Delta)\mu\partial_t\alpha_{2,5} - 2(9-2\Delta)\mu^2\alpha_{2,6}}{4(5-\Delta)}; \end{aligned} \quad (\text{B.26})$$

$$\begin{aligned} d_{(3)00} = & -\mu^{8-2\Delta} \frac{(\Delta-3)(7-2\Delta)\partial_t^3\alpha_{2,4} + 3(4-\Delta)(7-2\Delta)\mu\partial_t^2\alpha_{2,5}}{3(4\Delta^2-40\Delta+99)} \\ & + \mu^{8-2\Delta} \frac{(4-\Delta)\partial_t\alpha_{2,6} - 2(9-2\Delta)\mu^2((5-\Delta)\mu\alpha_{2,7})}{4\Delta^2-40\Delta+99}; \end{aligned} \quad (\text{B.27})$$

$$\begin{aligned} d_{(4)00} = & -\mu^{8-2\Delta} \frac{(2\Delta^3-25\Delta^2+107\Delta-162)\mu^4\alpha_{2,4}}{8(6-\Delta)(5-\Delta)} \\ & + \mu^{8-2\Delta} \frac{4(4-\Delta)(7-2\Delta)\mu\partial_t^3\alpha_{2,5} - 12(9-2\Delta)(4-\Delta)\mu^2\partial_t^2\alpha_{2,6}}{48(6-\Delta)(5-\Delta)} \\ & + \mu^{8-2\Delta} \frac{24(9-2\Delta)\mu^3\partial_t\alpha_{2,7} - 24(11-2\Delta)\mu^4\alpha_{2,8}}{48(6-\Delta)} \\ & + \mu^{8-2\Delta} \frac{(\Delta-3)(7-2\Delta)\partial_t^4\alpha_{2,4}}{48(6-\Delta)(5-\Delta)}, \end{aligned} \quad (\text{B.28})$$

where  $\alpha_{2,n}$  are the coefficients defined in eq. (3.11) — implicitly, functions of the FG time  $t$  here. Similarly, the coefficients in  $G_{ii}$  with factors of  $r^{-2\Delta}$  are given by

$$d_{(0)ii} = -\mu^{8-2\Delta} \frac{\alpha_{2,4} - 4(4-\Delta)\sigma_{2,5}}{2(4-\Delta)}; \quad (\text{B.29})$$

$$d_{(1)ii} = \mu^{8-2\Delta} \frac{\partial_t \alpha_{2,4} - 2(9-2\Delta)\partial_t \sigma_{2,5} - \mu\alpha_{2,5} + 2(9-2\Delta)\mu\sigma_{2,6}}{9-2\Delta}; \quad (\text{B.30})$$

$$d_{(2)ii} = -\mu^{8-2\Delta} \frac{\partial_t^2 \alpha_{2,4} - 4(5-\Delta)\partial_t^2 \sigma_{2,5}}{4(5-\Delta)} + \mu^{8-2\Delta} \frac{\mu\partial_t \alpha_{2,5} - 4(5-\Delta)\mu\partial_t \sigma_{2,6} - \mu^2 \alpha_{2,6} + 4(5-\Delta)\mu^2 \sigma_{2,7}}{2(5-\Delta)}; \quad (\text{B.31})$$

$$d_{(3)ii} = \frac{\mu^{8-2\Delta}}{6(11-2\Delta)} \left( \partial_t^3 \alpha_{2,4} - 2(11-2\Delta)\partial_t^3 \sigma_{2,5} - 3\mu\partial_t^2 \alpha_{2,5} + 6(11-2\Delta)\mu\partial_t^2 \sigma_{2,6} + \partial_t \alpha_{2,6} - 2(11-2\Delta)\partial_t \sigma_{2,7} - 6\mu^2 (\mu\alpha_{2,7} + 2(11-2\Delta)\mu\sigma_{2,8}) \right), \quad (\text{B.32})$$

where  $\sigma_{2,n}$  are the coefficients defined in (3.12) — implicitly, functions of the FG time  $t$  here.

The coefficients of the terms with factors of  $r^{2\Delta}$  in  $G_{00}$  are given by

$$e_{(0)00} = -\frac{(2\Delta-1)\mu^{2\Delta}\beta_{2,4}}{2\Delta}; \quad (\text{B.33})$$

$$e_{(1)00} = 2\mu^{2\Delta} \frac{(\Delta-1)\partial_t \beta_{2,4} - \Delta\mu\beta_{2,5}}{2\Delta+1}, \quad (\text{B.34})$$

where  $\beta_{2,n}$  is defined in eq. (3.11). Similarly, in  $G_{ii}$  the coefficients of the  $r^{2\Delta}$  are given by

$$e_{(0)ii} = -\mu^{2\Delta} \frac{\beta_{2,4} - 4\Delta\theta_{2,5}}{2\Delta}; \quad (\text{B.35})$$

$$e_{(1)ii} = \mu^{2\Delta} \frac{\partial_t \beta_{2,4} - 2(2\Delta+1)\partial_t \theta_{2,5} - \mu\beta_{2,5} + 2(2\Delta+1)\mu\tau_{2,6}}{2\Delta+1}, \quad (\text{B.36})$$

where  $\tau_{2,n}$  was defined in eq. (3.12).

### B.3 The scalar field

The coefficients of the scalar field  $f_{(n)}$  and  $g_{(n)}$  in the FG coordinates can be written in terms of the coefficients  $\phi_{(0)}$  and  $\phi_{(2\Delta-4)}$  in eq. (3.9). The coefficients of  $r^{4-\Delta}$  in  $\Phi_p$

are given by

$$\begin{aligned} \sum_{n=0} f_{(n)}(t)r^n &= \mu^{4-\Delta} \left( \phi_{(0)} + r\partial_t\phi_{(0)} - \frac{r^2(7-2\Delta)\partial_t^2\phi_{(0)}}{4(\Delta-3)} - \frac{r^3(9-2\Delta)\partial_t^3\phi_{(0)}}{12(\Delta-3)} \right. \\ &\quad \left. + r^4 \left( \frac{1}{8}(4-\Delta)\mu^4\phi_{(0)} - \frac{(4\Delta^2-40\Delta+99)\partial_t^4\phi_{(0)}}{96(4-\Delta)(\Delta-3)} \right) + o(r^5) \right), \end{aligned} \quad (\text{B.37})$$

while the only coefficient of  $r^\Delta$  that may play a role is

$$g_{(0)} = \mu^\Delta \phi_{(2\Delta-4)}. \quad (\text{B.38})$$

## C Boundary stress-energy tensor and $\langle \mathcal{O}_\Delta \rangle$

In section 5, we constructed the holographic action  $S_{reg} = S_{bulk} + S_{GHBV} + S_{count}$  which is now finite, *i.e.*, no divergences appear in the limit  $\epsilon \rightarrow 0$ . Hence, so are all quantities that can be calculated from this action. Of course, the latter includes the one-point functions of the stress tensor and operator  $\mathcal{O}_\Delta$ . In order to calculate these expectation values, we need to vary  $S_{reg}$  with respect to the boundary metric and the coupling to boundary operator, respectively. Recall that the boundary metric  $g_{ab}^{(0)}$  appears as the leading coefficient in the expansion (4.7) of the bulk metric. Similarly, the coupling  $\lambda$  is proportional to the leading coefficient  $f_{(0)}$  in the expansion (4.8) of the bulk scalar. We will establish our conventions for the precise normalization of the coupling in section 6.1 and so at this point, we simply introduce a dimensionless proportionality constant<sup>9</sup> with  $\ell f_{(0)} = \alpha_\lambda \lambda$ . Then the desired one-point functions are given by [24]

$$\begin{aligned} 8\pi G_N^{(5)} \langle T^{ab} \rangle &= \lim_{\epsilon \rightarrow 0} \frac{16\pi G_N^{(5)}}{\sqrt{-g^{(0)}}} \frac{\delta S_{reg}}{\delta g_{ab}^{(0)}} \\ &= \lim_{\epsilon \rightarrow 0} \frac{16\pi G_N^{(5)}}{\sqrt{-\gamma}\epsilon^4} \left( \frac{\delta S_{reg}}{\delta \gamma_{cd}} \frac{\delta \gamma_{cd}}{\delta g_{ab}^{(0)}} + \frac{\delta S_{reg}}{\delta \Phi} \frac{\delta \Phi}{\delta g_{ab}^{(0)}} \right) \end{aligned} \quad (\text{C.1})$$

and

$$\begin{aligned} 16\pi G_N^{(5)} \langle \mathcal{O}_\Delta \rangle &= \lim_{\epsilon \rightarrow 0} \frac{16\pi G_N^{(5)}}{\sqrt{-g^{(0)}}} \frac{\delta S_{reg}}{\delta \lambda} = \lim_{\epsilon \rightarrow 0} \frac{16\pi G_N^{(5)}}{\sqrt{-g^{(0)}}} \frac{\alpha_\lambda}{\ell} \frac{\delta S_{reg}}{\delta f_{(0)}} \\ &= \lim_{\epsilon \rightarrow 0} \frac{16\pi G_N^{(5)}}{\sqrt{-\gamma}\ell\epsilon^4} \left( \frac{\delta S_{reg}}{\delta \gamma_{ab}} \frac{\delta \gamma_{ab}}{\delta f_{(0)}} + \frac{\delta S_{reg}}{\delta \Phi} \frac{\delta \Phi}{\delta f_{(0)}} \right). \end{aligned} \quad (\text{C.2})$$

---

<sup>9</sup>The constant  $\alpha_\lambda$  is fixed in eq. (6.16).

We proceed by first evaluating the variations of the action with respect to  $\gamma$  and  $\Phi$ , then the variations of  $\gamma$  and  $\Phi$  with respect to  $g_{ab}^{(0)}$  and  $f_{(0)}$ . The variation of the action on the cut-off surface  $r = \epsilon$  is:

$$\begin{aligned}
\frac{16\pi G_N^{(5)}}{\sqrt{-\gamma}} \frac{\delta(S_{\text{bulk}} + S_{\text{GHBY}})}{\delta\gamma_{ab}} &= \frac{r}{2} \left( \gamma^{ac} \gamma^{bd} \partial_r \gamma_{cd} - \gamma^{ab} \gamma^{cd} \partial_r \gamma_{cd} \right) \Big|_{r=\epsilon}, \\
\frac{16\pi G_N^{(5)}}{\sqrt{-\gamma}} \frac{\delta(S_{\text{bulk}} + S_{\text{GHBY}})}{\delta\Phi} &= r \partial_r \Phi \Big|_{r=\epsilon}, \\
\frac{16\pi G_N^{(5)}}{\sqrt{-\gamma}} \frac{\delta S_{\text{count}}}{\delta\gamma_{ab}} &= -\frac{1}{2} \gamma^{ab} \left( 6 + \frac{4-\Delta}{2} \Phi^2 - \frac{1}{4(\Delta-3)} (\partial\Phi)^2 \right) \Big|_{r=\epsilon} \\
&\quad + \frac{1}{24(\Delta-3)} \left( (\nabla^a \nabla^b - \gamma^{ab} \square) \Phi^2 - 6 \gamma^{ac} \gamma^{bd} \partial_c \Phi \partial_d \Phi \right) \Big|_{r=\epsilon}, \\
\frac{16\pi G_N^{(5)}}{\sqrt{-\gamma}} \frac{\delta S_{\text{count}}}{\delta\Phi} &= -(4-\Delta) \Phi - \frac{1}{2(\Delta-3)} \square \Phi \Big|_{r=\epsilon}. \tag{C.3}
\end{aligned}$$

In the above we only showed the terms that would contribute at the orders of  $\ell$  we are considering. Using the results of appendix B, we find the variation of the bulk fields with respect to their boundary values (at leading order) are

$$\begin{aligned}
\frac{\delta\gamma_{cd}}{\delta g_{ab}^{(0)}} &= \delta_{(c}^a \delta_{d)}^b r^{-2} \Big|_{r=\epsilon}, & \frac{\delta\Phi}{\delta g_{ab}^{(0)}} &= o(r^{5-\Delta}), \\
\frac{\delta\gamma_{ab}}{\delta f_{(0)}} &= -\frac{1}{6} \eta_{ab} \ell^2 f_{(0)} r^{6-2\Delta} \Big|_{r=\epsilon}, & \frac{\delta\Phi}{\delta f_{(0)}} &= \ell r^{4-\Delta} \Big|_{r=\epsilon}. \tag{C.4}
\end{aligned}$$

The second equation in eq. (C.4) leads to a vanishing contribution to the stress tensor in eq. (C.1). The third equation above only contributes to eq. (C.2) when  $\Delta = 4$  and hence can be ignored for our purposes. Inserting the variations from eqs. (C.3) and (C.4) into eqs. (C.1) and (C.2), we get the results presented in the main text in eqs. (5.4)–(5.6). Note that for these final results, we have replaced  $f_{(0)}$  and  $g_{(0)}$  by their expressions in terms of  $\phi_{(0)}$  and  $\phi_{(2\Delta-4)}$  given in appendix B.3.

## References

- [1] For example, see the following reviews:  
S. Mondal, D. Sen and K. Sengupta, “Non-equilibrium dynamics of quantum systems: order parameter evolution, defect generation, and qubit transfer,” *Quantum Quenching, Annealing and Computation*, Lecture notes in Physics, Volume 802, Page 21, 2010 [arXiv:0908.2922[cond-mat.stat-mech]];

- J. Dziarmaga, “Dynamics of a quantum phase transition and relaxation to a steady state,” *Adv. Phys.* **59**, 1063 (2010) [arXiv:0912.4034 [cond-mat.quant-gas]];
- A. Polkovnikov, K. Sengupta, A. Silva and M. Vengalattore, “Nonequilibrium dynamics of closed interacting quantum systems,” *Rev. Mod. Phys.* **83**, 863 (2011) [arXiv:1007.5331 [cond-mat.stat-mech]];
- A. Lamacraft and J.E. Moore, “Potential insights into non-equilibrium behavior from atomic physics,” Chapter forthcoming in *Ultracold Bosonic and Fermionic Gases*, Contemporary Concepts in Condensed Matter Science, Elsevier (Editors: A. Fletcher, K. Levin and D. Stamper-Kurn) [arXiv:1106.3567[cond-mat.quant-gas]].
- [2] L. D. Landau and E. M. Lifshitz, *Quantum Mechanics*, Course of Theoretical Physics, Volume 3, 1989.
- [3] P. Calabrese and J. L. Cardy, “Evolution of entanglement entropy in one-dimensional systems,” *J. Stat. Mech.* **0504**, P04010 (2005) [cond-mat/0503393];
- P. Calabrese and J. L. Cardy, “Time-dependence of correlation functions following a quantum quench,” *Phys. Rev. Lett.* **96**, 136801 (2006) [cond-mat/0601225];
- P. Calabrese and J. Cardy, “Quantum Quenches in Extended Systems,” *J. Stat. Mech.* **0706**, P06008 (2007) [arXiv:0704.1880 [cond-mat.stat-mech]];
- S. Sotiriadis and J. Cardy, “Quantum quench in interacting field theory: A Self-consistent approximation,” *Phys. Rev. B* **81**, 134305 (2010) [arXiv:1002.0167 [quant-ph]];
- S. Sotiriadis and J. Cardy, “Inhomogeneous Quantum Quenches,” *J. Stat. Mech.* P11003 (2008) [arXiv:0808.0116 [cond-mat.stat-mech]];
- S. Sotiriadis, P. Calabrese and J. Cardy, “Quantum quench from a thermal initial state,” *EPL* **87**, 20002 (2009) [arXiv:0903.0895v2 [cond-mat.stat-mech]].
- [4] M. Rigol, V. Dunjko, V. Yurovsky, and M. Olshanii, “Relaxation in a completely integrable many-body quantum system: An ab initio study of the dynamics of the highly excited states of lattice hard-core bosons”, *Phys. Rev. Lett.* **98** (2006), no. 5 4;
- C. Kollath, A. Laeuchli, and E. Altman, “Quench dynamics and nonequilibrium phase diagram of the bose-hubbard model”, *Phys. Rev. Lett.* **98** (2006), no. 18 180601;
- S. R. Manmana, S. Wessel, R. M. Noack, and A. Muramatsu, “Strongly correlated

- fermions after a quantum quench”, *Phys. Rev. Lett.* **98** (2006), no. 21 4;  
 L. -Y. Hung, M. Smolkin and E. Sorkin, “Modification of late time phase structure by quantum quenches,” *arXiv:1206.2685* [cond-mat.str-el].
- [5] J. M. Maldacena, “The large N limit of superconformal field theories and supergravity,” *Adv. Theor. Math. Phys.* **2**, 231 (1998) [*Int. J. Theor. Phys.* **38**, 1113 (1999)] [*arXiv:hep-th/9711200*];  
 O. Aharony, S. S. Gubser, J. M. Maldacena, H. Ooguri and Y. Oz, “Large N field theories, string theory and gravity,” *Phys. Rept.* **323**, 183 (2000) [*arXiv:hep-th/9905111*].
- [6] S. R. Das, T. Nishioka and T. Takayanagi, “Probe Branes, Time-dependent Couplings and Thermalization in AdS/CFT,” *JHEP* **1007**, 071 (2010) [*arXiv:1005.3348* [hep-th]];  
 P. Basu and S. R. Das, “Quantum Quench across a Holographic Critical Point,” *JHEP* **1201**, 103 (2012) [*arXiv:1109.3909* [hep-th]];  
 S. R. Das, “Holographic Quantum Quench,” *J. Phys. Conf. Ser.* **343**, 012027 (2012) [*arXiv:1111.7275* [hep-th]];  
 P. Basu, D. Das, S. R. Das and T. Nishioka, “Quantum Quench Across a Zero Temperature Holographic Superfluid Transition,” *arXiv:1211.7076* [hep-th].
- [7] U. H. Danielsson, E. Keski-Vakkuri and M. Kruczenski, “Spherically collapsing matter in AdS, holography, and shellons,” *Nucl. Phys. B* **563**, 279 (1999) [*hep-th/9905227*];  
 U.H. Danielsson, E. Keski-Vakkuri and M. Kruczenski, “Black hole formation in AdS and thermalization on the boundary,” *JHEP* **0002**, 039 (2000) [*hep-th/9912209*];  
 S.B. Giddings and S.F. Ross, “D3-brane shells to black branes on the Coulomb branch,” *Phys. Rev. D* **61**, 024036 (2000) [*hep-th/9907204*];  
 S. B. Giddings and A. Nudelman, “Gravitational collapse and its boundary description in AdS,” *JHEP* **0202**, 003 (2002) [*hep-th/0112099*];  
 S. Bhattacharyya and S. Minwalla, “Weak Field Black Hole Formation in Asymptotically AdS Spacetimes,” *JHEP* **0909**, 034 (2009) [*arXiv:0904.0464* [hep-th]].  
 R. A. Janik and R. B. Peschanski, “Gauge/gravity duality and thermalization of a boost-invariant perfect fluid,” *Phys. Rev. D* **74**, 046007 (2006) [*hep-th/0606149*];  
 R. A. Janik, “Viscous plasma evolution from gravity using AdS/CFT,” *Phys. Rev.*



- Lett. **98**, 022302 (2007) [hep-th/0610144];
- S. Lin and E. Shuryak, “Toward the AdS/CFT Gravity Dual for High Energy Collisions. 3. Gravitationally Collapsing Shell and Quasiequilibrium,” Phys. Rev. D **78**, 125018 (2008) [arXiv:0808.0910 [hep-th]].
- [8] J. Abajo-Arrastia, J. Aparicio and E. Lopez, “Holographic Evolution of Entanglement Entropy,” JHEP **1011**, 149 (2010) [arXiv:1006.4090 [hep-th]];
- T. Albash and C. V. Johnson, “Evolution of Holographic Entanglement Entropy after Thermal and Electromagnetic Quenches,” New J. Phys. **13**, 045017 (2011) [arXiv:1008.3027 [hep-th]];
- H. Ebrahim and M. Headrick, “Instantaneous Thermalization in Holographic Plasmas,” arXiv:1010.5443 [hep-th];
- V. Balasubramanian *et al.*, “Thermalization of Strongly Coupled Field Theories,” Phys. Rev. Lett. **106**, 191601 (2011) [arXiv:1012.4753 [hep-th]];
- V. Balasubramanian *et al.*, “Holographic Thermalization,” Phys. Rev. D **84**, 026010 (2011) [arXiv:1103.2683 [hep-th]];
- V. Balasubramanian, A. Bernamonti, N. Copland, B. Craps and F. Galli, “Thermalization of mutual and tripartite information in strongly coupled two dimensional conformal field theories,” Phys. Rev. D **84**, 105017 (2011) [arXiv:1110.0488 [hep-th]];
- J. Aparicio and E. Lopez, “Evolution of Two-Point Functions from Holography,” JHEP **1112**, 082 (2011) [arXiv:1109.3571 [hep-th]];
- A. Allais and E. Tonni, “Holographic evolution of the mutual information,” JHEP **1201**, 102 (2012) [arXiv:1110.1607 [hep-th]];
- V. Keranen, E. Keski-Vakkuri and L. Thorlacius, “Thermalization and entanglement following a non-relativistic holographic quench,” Phys. Rev. D **85**, 026005 (2012) [arXiv:1110.5035 [hep-th]];
- D. Galante and M. Schvellinger, “Thermalization with a chemical potential from AdS spaces,” JHEP **1207**, 096 (2012) [arXiv:1205.1548 [hep-th]];
- E. Caceres and A. Kundu, “Holographic Thermalization with Chemical Potential,” JHEP **1209**, 055 (2012) [arXiv:1205.2354 [hep-th]];
- I. Y. Arefeva and I. V. Volovich, “On Holographic Thermalization and Dethermalization of Quark-Gluon Plasma,” arXiv:1211.6041 [hep-th];
- W. H. Baron, D. Galante and M. Schvellinger, “Dynamics of holographic thermalization,” arXiv:1212.5234 [hep-th].

- [9] P.M. Chesler and L.G. Yaffe, “Horizon formation and far-from-equilibrium isotropization in supersymmetric Yang-Mills plasma,” *Phys. Rev. Lett.* **102**, 211601 (2009). [arXiv:0812.2053 [hep-th]];  
P. M. Chesler and L. G. Yaffe, “Boost invariant flow, black hole formation, and far-from-equilibrium dynamics in  $N = 4$  supersymmetric Yang-Mills theory,” *Phys. Rev. D* **82**, 026006 (2010) [arXiv:0906.4426 [hep-th]].
- [10] D. Garfinkle and L. A. Pando Zayas, “Rapid Thermalization in Field Theory from Gravitational Collapse,” *Phys. Rev. D* **84**, 066006 (2011) [arXiv:1106.2339 [hep-th]];  
D. Garfinkle, L. A. Pando Zayas and D. Reichmann, “On Field Theory Thermalization from Gravitational Collapse,” *JHEP* **1202**, 119 (2012) [arXiv:1110.5823 [hep-th]];  
H. Bantilan, F. Pretorius and S. S. Gubser, “Simulation of Asymptotically AdS5 Spacetimes with a Generalized Harmonic Evolution Scheme,” *Phys. Rev. D* **85**, 084038 (2012) [arXiv:1201.2132 [hep-th]];  
M. P. Heller, D. Mateos, W. van der Schee and D. Trancanelli, “Strong Coupling Isotropization of Non-Abelian Plasmas Simplified,” *Phys. Rev. Lett.* **108**, 191601 (2012) [arXiv:1202.0981 [hep-th]];  
M. P. Heller, R. A. Janik and P. Witaszczyk, “A numerical relativity approach to the initial value problem in asymptotically Anti-de Sitter spacetime for plasma thermalization – an ADM formulation,” *Phys. Rev. D* **85**, 126002 (2012) [arXiv:1203.0755 [hep-th]];  
M. J. Bhaseen, J. P. Gauntlett, B. D. Simons, J. Sonner and T. Wiseman, “Holographic Superfluids and the Dynamics of Symmetry Breaking,” *Phys. Rev. Lett.* **110**, 015301 (2013) [arXiv:1207.4194 [hep-th]];  
B. Wu, “On holographic thermalization and gravitational collapse of massless scalar fields,” *JHEP* **1210**, 133 (2012) [arXiv:1208.1393 [hep-th]];  
B. Wu, “On holographic thermalization and gravitational collapse of tachyonic scalar fields,” arXiv:1301.3796 [hep-th].
- [11] V. Cardoso, L. Gualtieri, C. Herdeiro, U. Sperhake, P. M. Chesler, L. Lehner, S. C. Park, H. S. Reall *et al.*, “NR/HEP: roadmap for the future,” *Class. Quant. Grav.* **29**, 244001 (2012). [arXiv:1201.5118 [hep-th]].

- [12] A. Buchel, L. Lehner and R. C. Myers, “Thermal quenches in  $N=2^*$  plasmas,” JHEP **1208**, 049 (2012) [arXiv:1206.6785 [hep-th]].
- [13] E. Witten, “Anti-de Sitter space, thermal phase transition, and confinement in gauge theories,” Adv. Theor. Math. Phys. **2**, 505 (1998) [hep-th/9803131].
- [14] S. S. Gubser, I. R. Klebanov and A. M. Polyakov, “Gauge theory correlators from noncritical string theory,” Phys. Lett. B **428**, 105 (1998) [hep-th/9802109];  
E. Witten, “Anti-de Sitter space and holography,” Adv. Theor. Math. Phys. **2**, 253 (1998) [hep-th/9802150].
- [15] P. Breitenlohner and D. Z. Freedman, “Positive Energy In Anti-De Sitter Backgrounds And Gauged Extended Supergravity,” Phys. Lett. B **115**, 197 (1982);  
P. Breitenlohner and D. Z. Freedman, “Stability In Gauged Extended Supergravity,” Annals Phys. **144**, 249 (1982);  
L. Mezincescu and P. K. Townsend, “Stability At A Local Maximum In Higher Dimensional Anti-De Sitter Space And Applications To Supergravity,” Annals Phys. **160**, 406 (1985).
- [16] I. R. Klebanov and E. Witten, “AdS/CFT correspondence and symmetry breaking,” Nucl. Phys. B **556**, 89 (1999) [arXiv:hep-th/9905104].
- [17] A. Buchel, J. Escobedo, R. C. Myers, M. F. Paulos, A. Sinha and M. Smolkin, “Holographic GB gravity in arbitrary dimensions,” JHEP **1003**, 111 (2010) [arXiv:0911.4257 [hep-th]].
- [18] S. Bhattacharyya, V. E. Hubeny, S. Minwalla and M. Rangamani, “Nonlinear Fluid Dynamics from Gravity,” JHEP **0802**, 045 (2008) [arXiv:0712.2456 [hep-th]];  
V. E. Hubeny, S. Minwalla and M. Rangamani, “The fluid/gravity correspondence,” Chapter in *Black holes in Higher Dimensions*, To be published by Cambridge University Press (Editor: G. Horowitz) [arXiv:1107.5780 [hep-th]].
- [19] R. Emparan, C. V. Johnson and R. C. Myers, “Surface terms as counterterms in the AdS/CFT correspondence,” Phys. Rev. D **60**, 104001 (1999) [hep-th/9903238].
- [20] M. Henningson and K. Skenderis, “The Holographic Weyl anomaly,” JHEP **9807**, 023 (1998) [hep-th/9806087].

- [21] M. Bianchi, D. Z. Freedman and K. Skenderis, “Holographic renormalization,” Nucl. Phys. B **631**, 159 (2002) [arXiv:hep-th/0112119];  
M. Bianchi, D. Z. Freedman and K. Skenderis, “How to go with an RG flow,” JHEP **0108**, 041 (2001) [arXiv:hep-th/0105276].
- [22] C. Fefferman and C. R. Graham, “Conformal Invariants,” in *Elie Cartan et les Mathématiques d’aujourd’hui* (Astérisque, 1985) 95;  
C. Fefferman and C. R. Graham, “The Ambient Metric,” arXiv:0710.0919 [math.DG].
- [23] L.-Y. Hung, R. C. Myers and M. Smolkin, “Some Calculable Contributions to Holographic Entanglement Entropy,” JHEP **1108**, 039 (2011) [arXiv:1105.6055 [hep-th]].
- [24] O. Aharony, A. Buchel and A. Yarom, “Holographic renormalization of cascading gauge theories,” Phys. Rev. D **72**, 066003 (2005) [hep-th/0506002].
- [25] I. Papadimitriou, “Holographic Renormalization of general dilaton-axion gravity,” JHEP **1108**, 119 (2011) [arXiv:1106.4826 [hep-th]].
- [26] A. Buchel, “N=2\* hydrodynamics,” Nucl. Phys. B **708**, 451 (2005) [hep-th/0406200].
- [27] A. Buchel and J. T. Liu, “Thermodynamics of the N=2\* flow,” JHEP **0311**, 031 (2003) [hep-th/0305064].
- [28] P. M. Hohler and M. A. Stephanov, “Holography and the speed of sound at high temperatures,” Phys. Rev. D **80**, 066002 (2009) [arXiv:0905.0900 [hep-th]].
- [29] R. A. Isaacson, J. S. Welling and J. Winicour, “Null Cone Computation Of Gravitational Radiation,” J. Math. Phys. **24**, 1824 (1983).
- [30] L. Lehner, “A Dissipative algorithm for wave - like equations in the characteristic formulation,” J. Comput. Phys. **149**, 1 (1999) [gr-qc/9811095].
- [31] A. Buchel, L. Lehner, R. C. Myers and A. van Niekerk, in preparation.